Original research

A revised Gaussian pencil beam model for calculation of the in-water dose caused by clinical electron-beam irradiation

Akira Iwasaki, Shingo Terashima, Shigenobu Kimura, Kohji Sutoh, Kazuo Kamimura, Yoichiro Hosokawa, Masanori Miyazawa , and Tatsuo Tabata

http://dx.doi.org/10.14312/2399-8172.2022-1

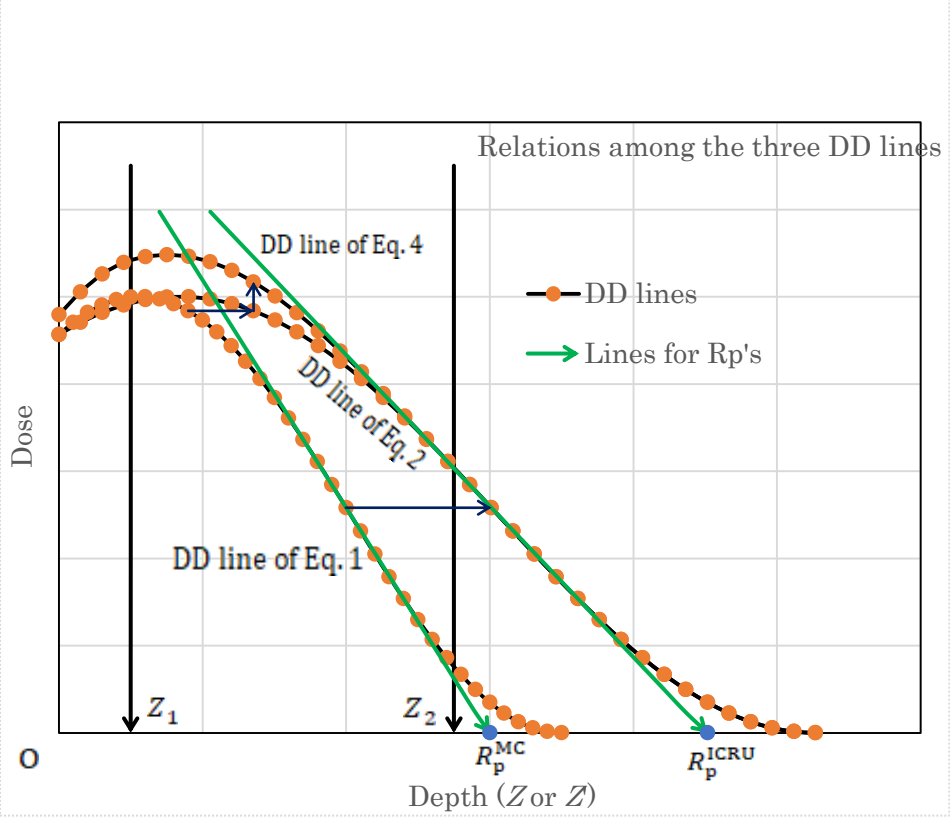

Supplementary Figure 1 Diagram showing how to obtain the final depth-dose curve $D_{\mathrm{para}}(0,0,Z{:}A_0=\infty)$ of Eq. 4 via the depth-dose curve of $D'_{\mathrm{para}}(0,0,Z{:}A_0=\infty)$ of Eq. 2 that is yielded from the depth-dose curve $D'_{\mathrm{para}}(0,0,Z'{:}A_0)$ of Eq. 1 using the relation of$Z=Z'\times\left(R_{\mathrm{p}}^{\mathrm{ICRU}}/R_{\mathrm{p}}^{\mathrm{MC}}\right)$. It should also be noted that the final depth-dose curve $D_{\mathrm{para}}(0,0,Z{:}A_0=\infty)$ is yielded by modifying the depth-dose curve of $D'_{\mathrm{para}}(0,0,Z{:}A_0=\infty)$ in Eq. 4 by using the three factors of $\mathrm{FAC}_{\mathrm{adjust}}$ (Supplementary Tables 1 and 2), FAC_1 (Eqs. 5a & 5b), and FAC_2 (Eqs. 6-8).

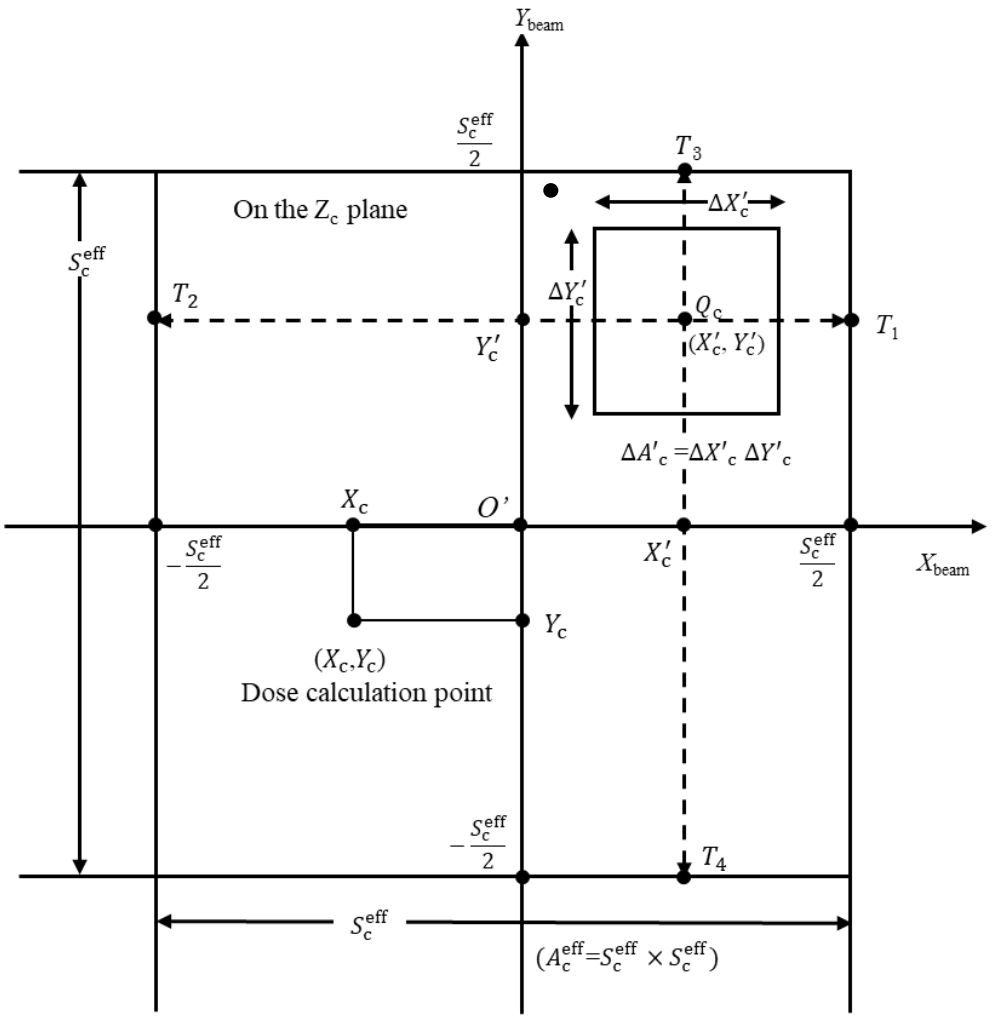

Supplementary Figure 2 Diagram showing how the geometric symbols are used for calculation of the $\mathrm{FAC}_1(T_{\min}: Z_c, A_c^{\mathrm{eff}})$ factor for point (X'_c, Y'_c), where the whole of $\Delta A'_c = \Delta X'_c \Delta Y'_c$ is set inside the field of $A_c^{\mathrm{eff}} = S_c^{\mathrm{eff}} \times S_c^{\mathrm{eff}}$ on the Z_c plane. It should be noted that $T_{\min}$ expresses the minimum among the values of (T_1, T_2, T_3, T_4), expressing the distances to each of the four square sides of A_c^{eff} from point (X'_c, Y'_c). The dose calculation point (X_c, Y_c) may be set at any position on the Z_c plane.

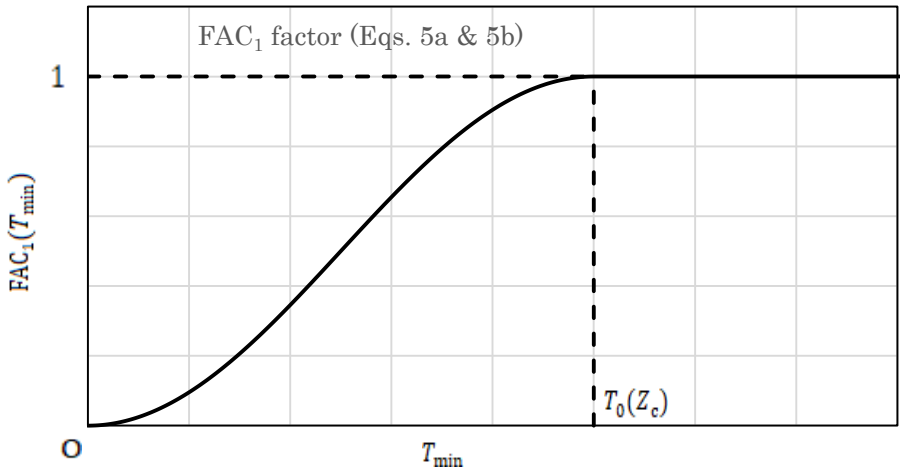

Supplementary Figure 3 Diagram showing how $\mathrm{FAC}_1(T_{\mathrm{min}}: Z_c, A_c^{\mathrm{eff}})$ varies with T_{min} for a given value of $T_0(Z_c: A_c^{\mathrm{eff}})$.

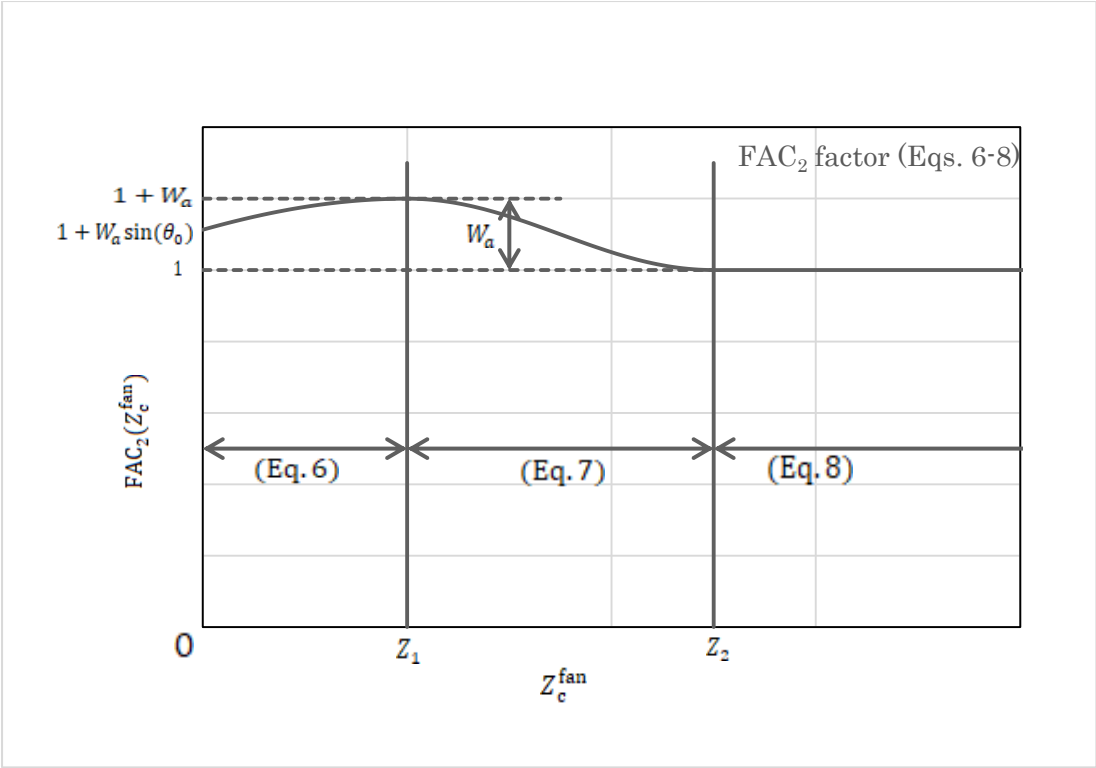

Supplementary Figure 4 Diagram showing how $\mathrm{FAC}_2(Z_c^{\mathrm{fan}}; Z_c, A_c^{\mathrm{eff}})$ varies with Z_c^{fan} using Eqs. 6-8.

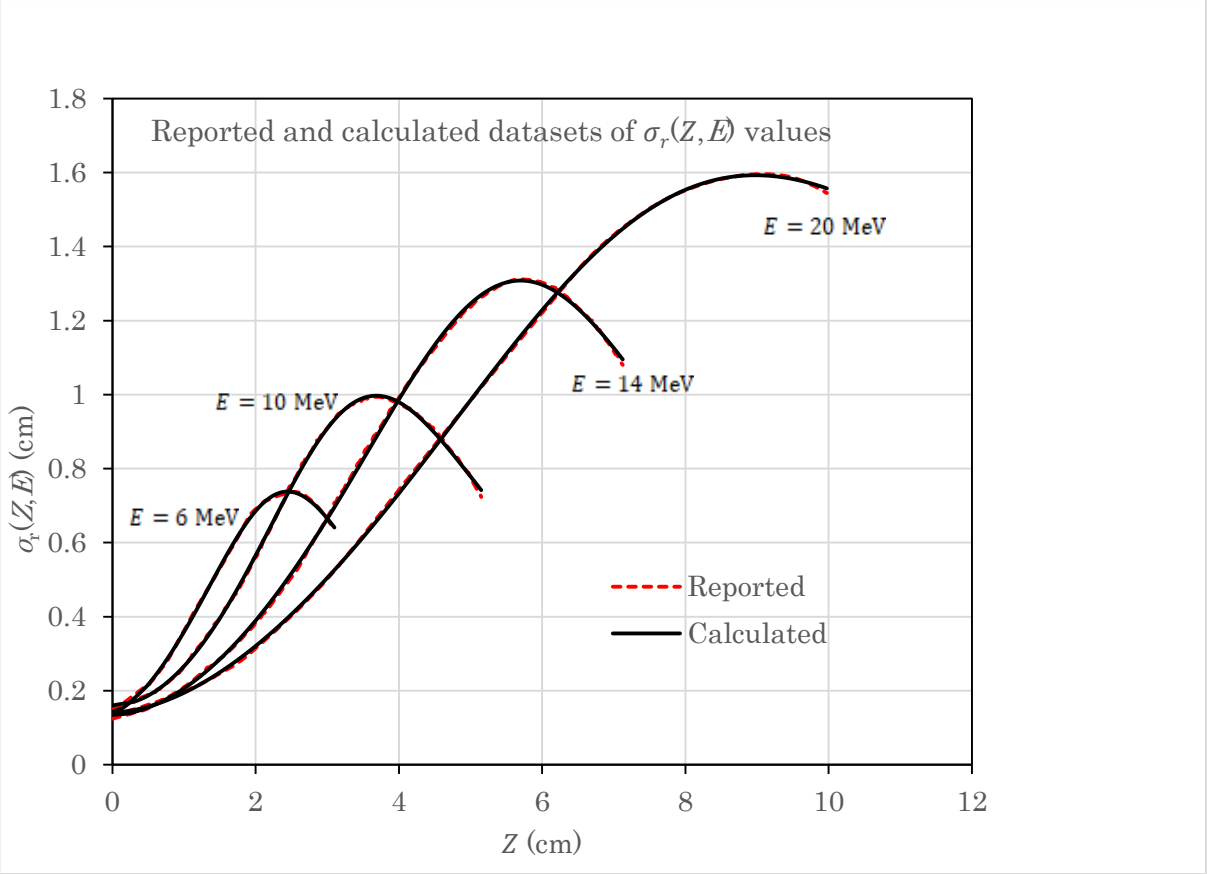

Supplementary Figure 5 Dependence of the $\sigma_r(Z, E)$ function on depth (Z) for each of E=6, 10, 14, and 20 MeV electron beams. Solid curves show Eq. 13 with the corresponding sets of $a(E)$-$e(E)$ values in Supplementary Table 2. Broken curves are the data reported by Bruinvis *et al*.

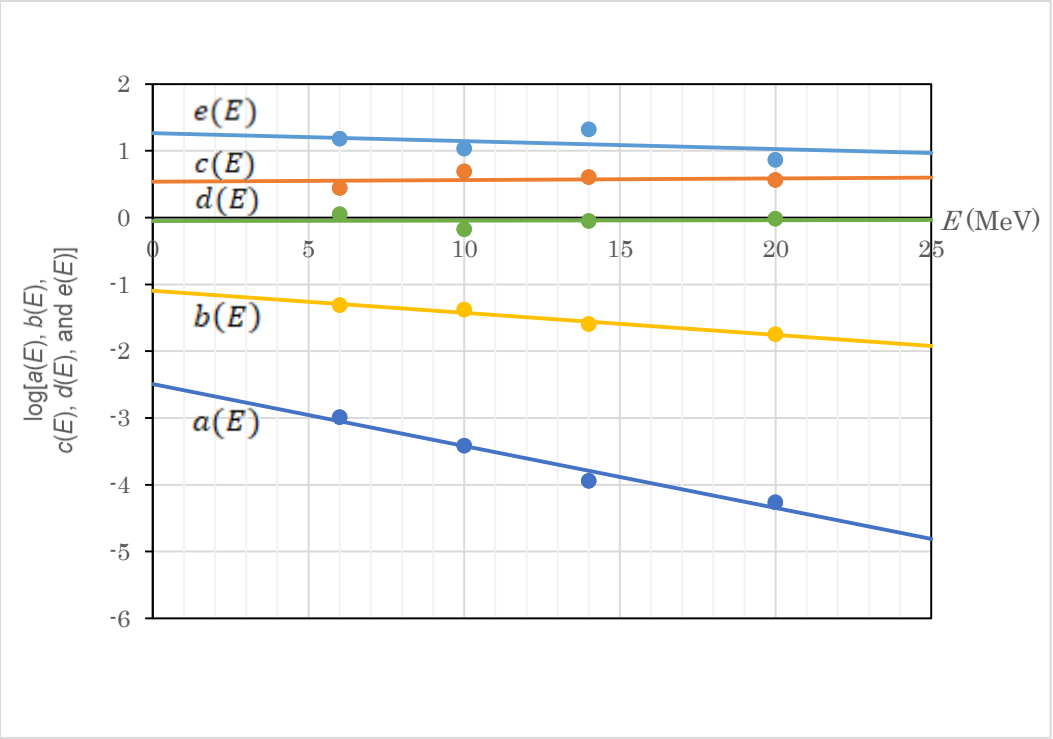

Supplementary Figure 6 Dependence of the log[*a*(*E*)], log[*b*(*E*)], log[*c*(*E*)], log[*d*(*E*)], and log[*e*(*E*)] functions on *E*. Straight lines show Eqs. 15-19; and dots, the corresponding datasets of $a(E)$-$e(E)$ in Table 2. Relatively large differences between the equation and dataset arise for the $e(E)$ function.

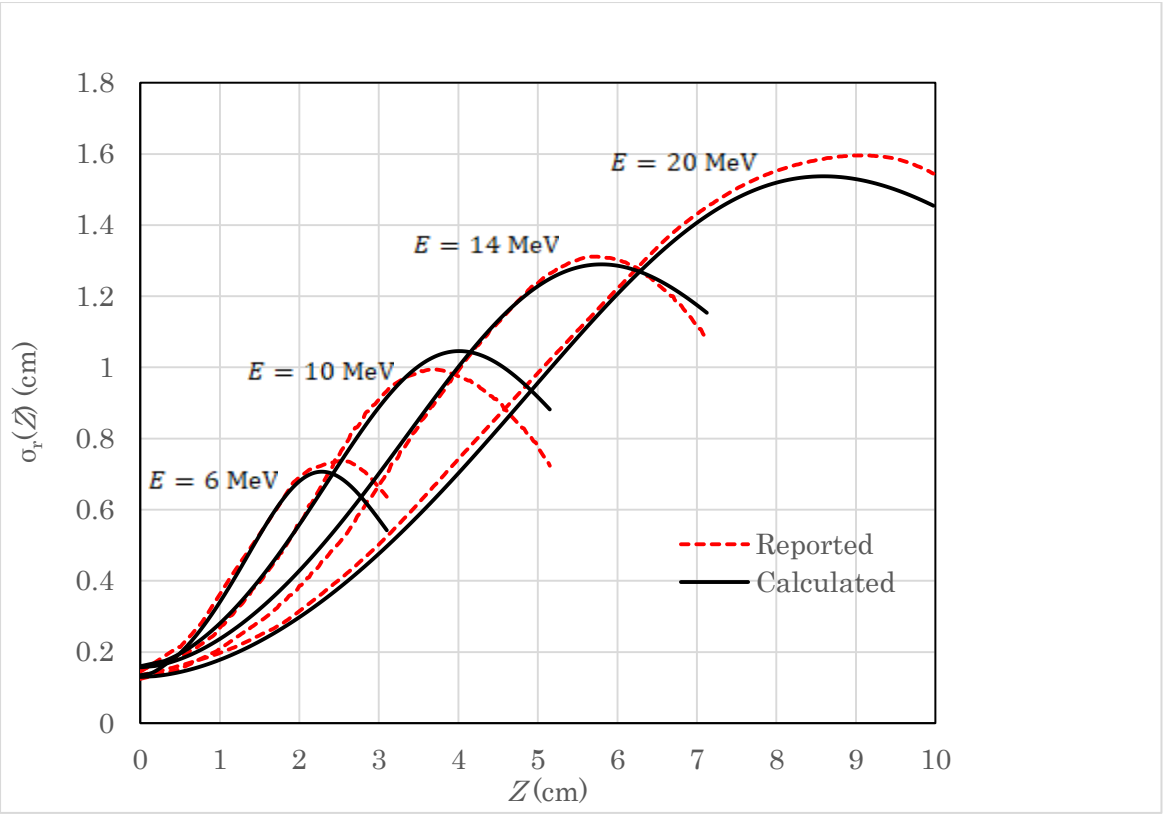

Supplementary Figure 7 Dependence of the $\sigma_r(Z)$ functions on depth (Z) for E=6, 10, 14, and 20 MeV. The solid curves show the generalized formula, Eq. 13 with Eqs. 15-19. The broken curves are the data reported by Bruinvis et al.

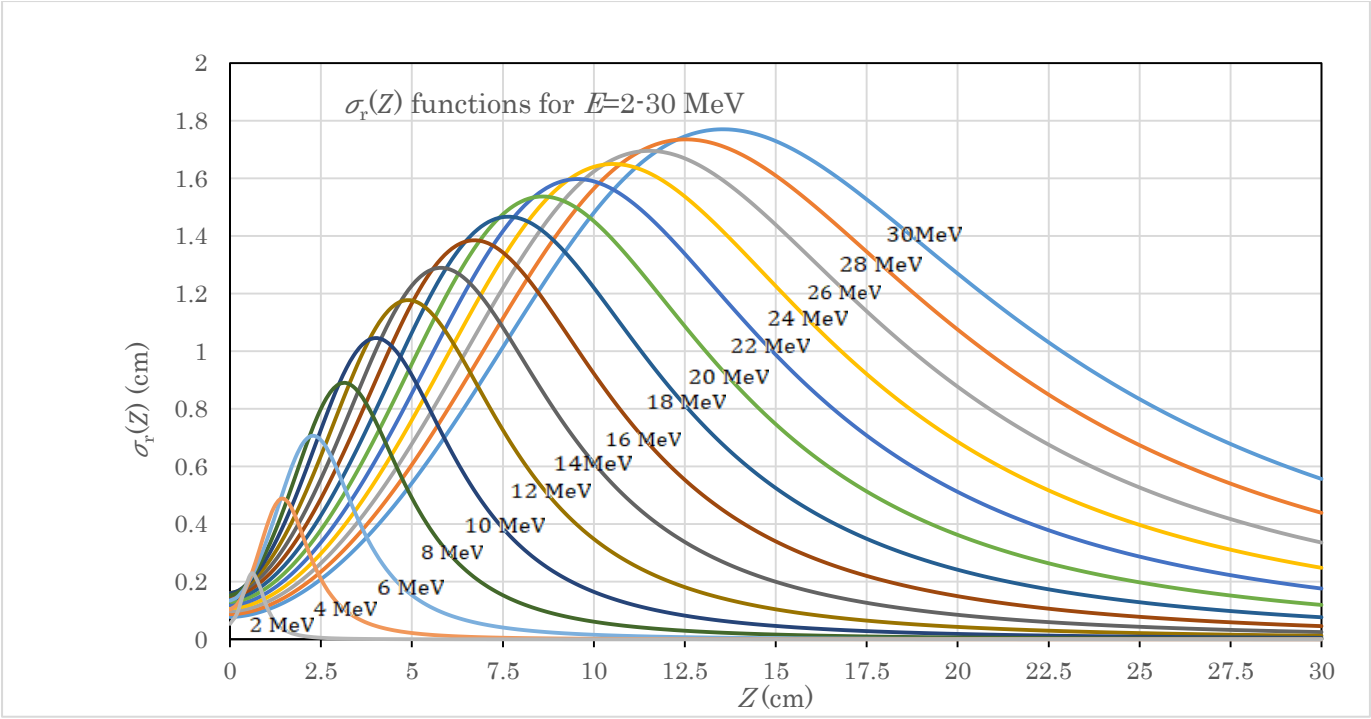

Supplementary Figure 8 Diagram showing the curves of $\sigma_r(Z)$ generated using Eq. 13 with the $a(E)$-$e(E)$ functions of Eqs. 15-19 for E =2-30 MeV at intervals of 2 MeV.

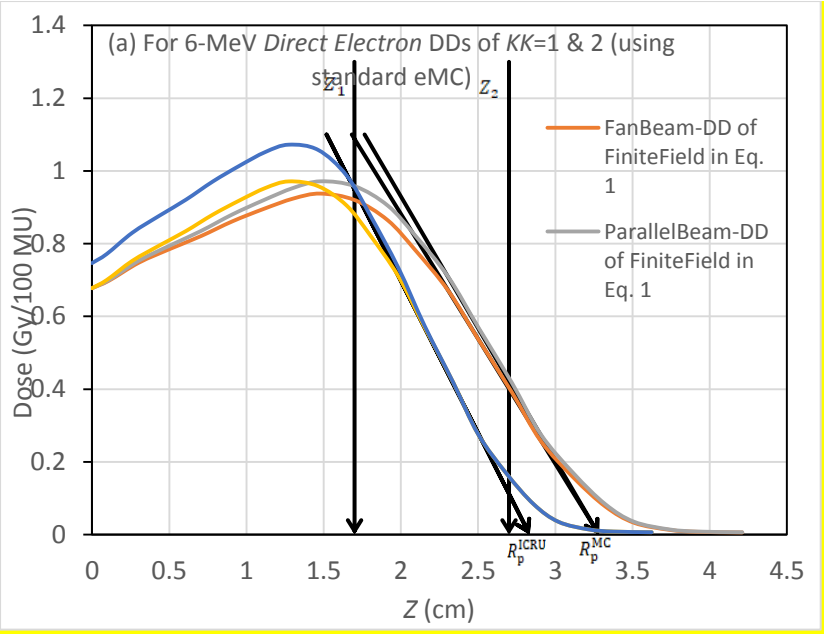
(a) For 6-MeV *Direct Electron* DDs of *KK*=1 & 2 (using standard eMC)
Z_1
Z_2
FanBeam-DD of FiniteField in Eq. 1
ParallelBeam-DD of FiniteField in Eq. 1
Dose (Gy/100 MU)
R_p^{ICRU}
R_p^{MC}
Z (cm)

(a)

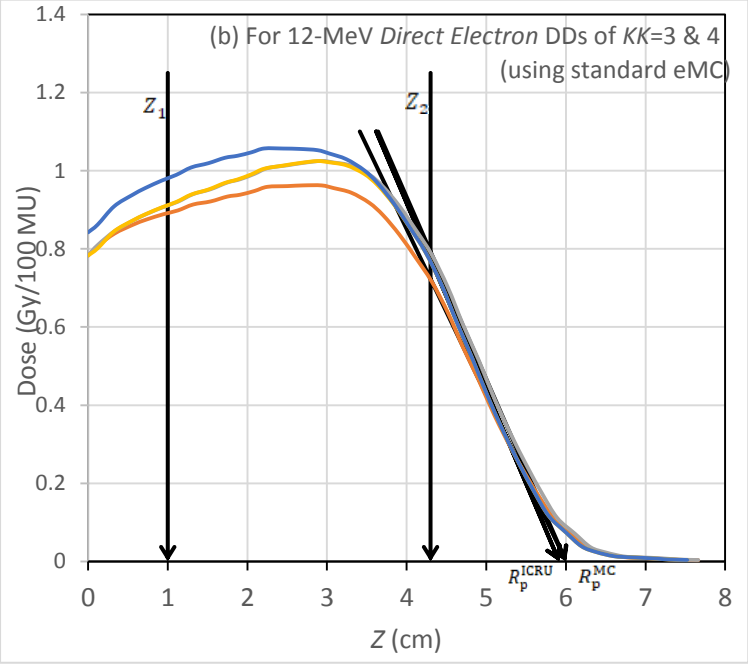
(b) For 12-MeV *Direct Electron* DDs of *KK*=3 & 4 (using standard eMC)
Z_1
Z_2
Dose (Gy/100 MU)
R_p^{ICRU}
R_p^{MC}
Z (cm)

(b)

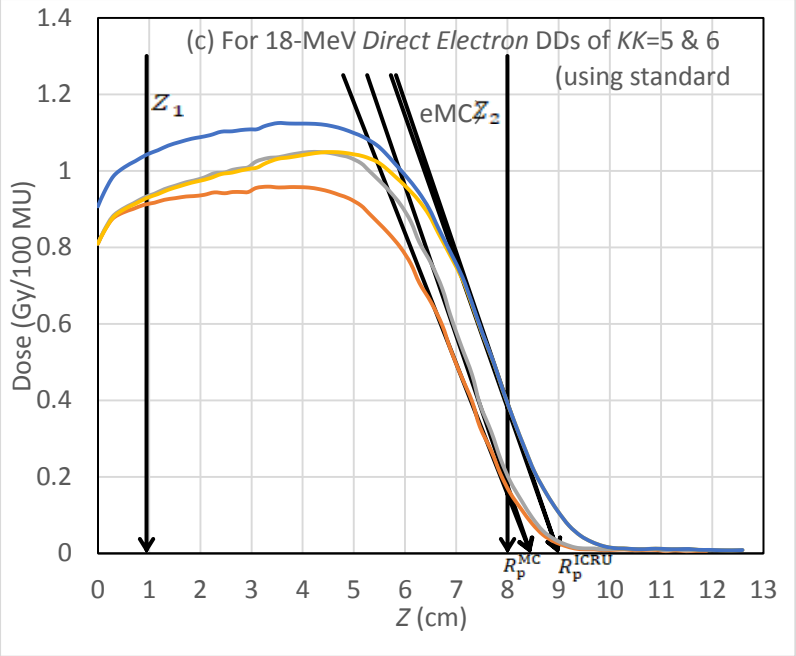

(c)

Supplementary Figure 9a-c Each of (a)-(c) diagrams showing a series of DD curves yielded using the standard eMC, reaching the corresponding parallel beam DD curve of infinite field ($A_0 = \infty$) used for direct electron beams, derived on the basis of the stepped DD-curves in (a) *Supp. fig. 1(a)* showing 6-MeV DD (*KK*=1 and 2), (b) *Supp. fig. 3(a)* showing 12-MeV DD (*KK*=3 and 4), and (c) *Supp. fig. 1(d)* showing 18-MeV DD (*KK*=5 and 6), as listed in Supplementary Table 1. In each DD group of (a)-(c), the first DD shows $D_{\text{fan}}(0,0,Z = Z' : A_0)$ in Eq. 1 (orange line), the second DD shows $D'_{\text{para}}(0,0,Z = Z' : A_0)$ in Eq. 1 (gray line), the third DD shows $D'_{\text{para}}(0,0,Z : A_0 = \infty)$ in Eq. 2 (yellow line), and the last DD shows $D_{\text{para}}\left(0,0,Z = Z_c^{\text{fan}} : A_0 = \infty\right)$ of Eq. 4 (blue line).

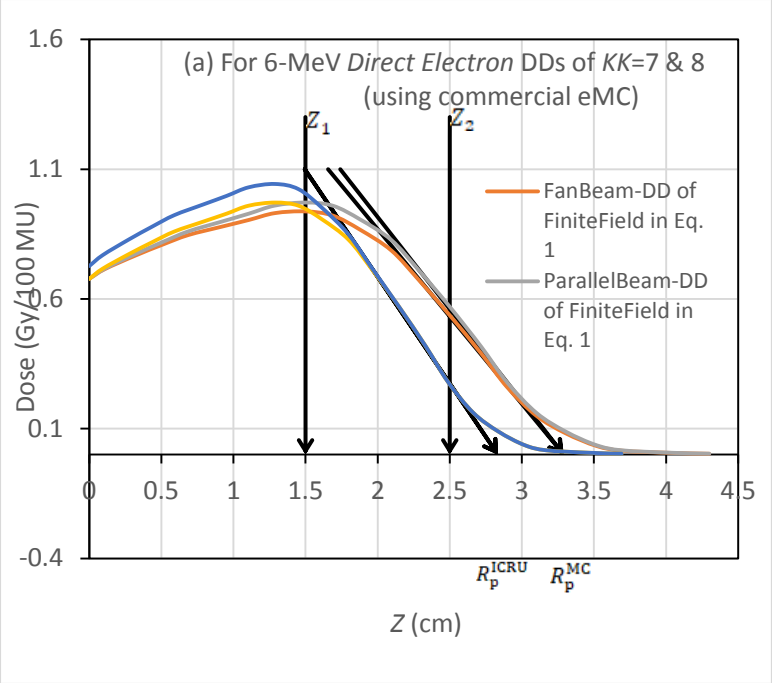
(a) For 6-MeV *Direct Electron* DDs of *KK*=7 & 8
(using commercial eMC)
Z_1
Z_2
FanBeam-DD of FiniteField in Eq. 1
ParallelBeam-DD of FiniteField in Eq. 1
Dose (Gy/100 MU)
1.6
1.1
0.6
0.1
-0.4
0
0.5
1
1.5
2
2.5
3
3.5
4
4.5
R_p^{ICRU}
R_p^{MC}
Z (cm)

(a)

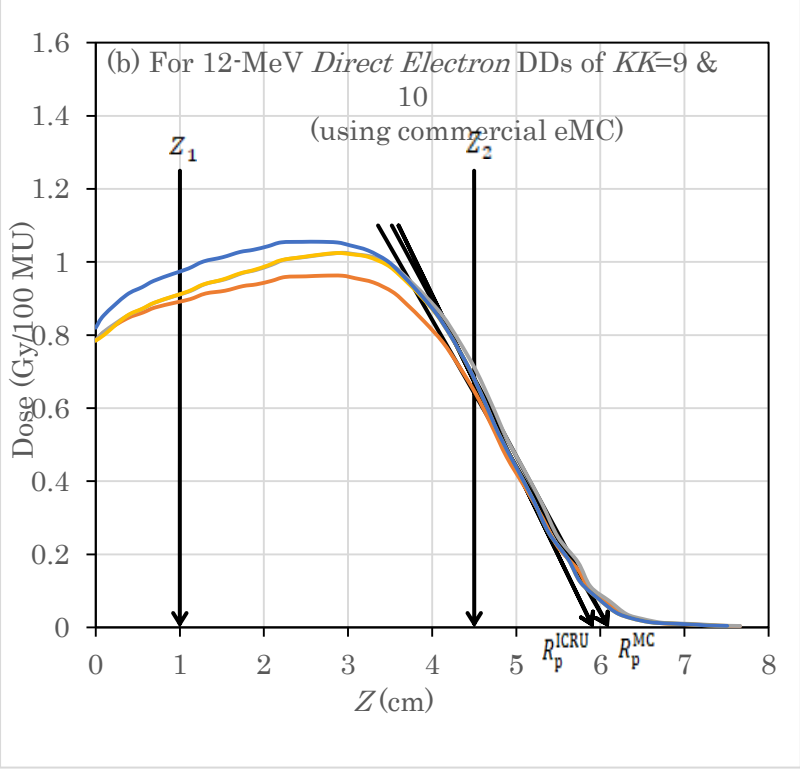
(b) For 12-MeV *Direct Electron* DDs of *KK*=9 & 10
(using commercial eMC)
Z_1
Z_2
Dose (Gy/100 MU)
1.6
1.4
1.2
1
0.8
0.6
0.4
0.2
0
0
1
2
3
4
5
6
7
8
R_p^{ICRU}
R_p^{MC}
Z (cm)

(b)

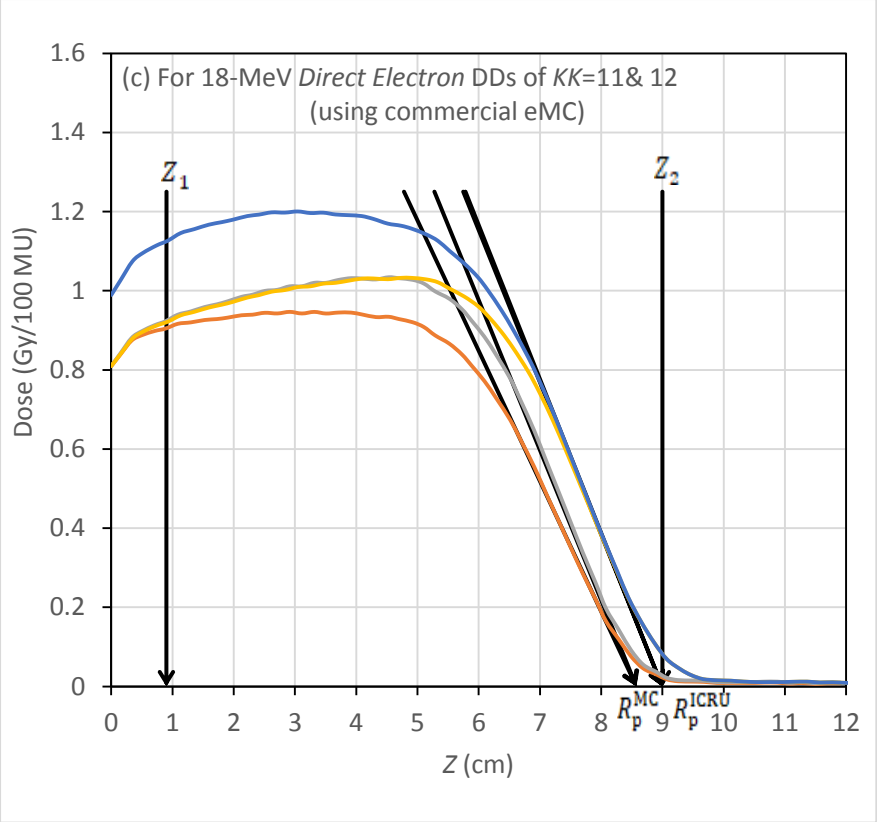

(c)

Supplementary Figure 10a-c Each of (a)-(c) diagrams showing a series of DD curves yielded using the commercial eMC, reaching the corresponding parallel beam DD curve of infinite field ($A_0 = \infty$) used for direct electron beams, derived on the basis of the dotted DD-curves in (a) *Supp. fig. 1(a)* showing 6-MeV DD (*KK*=7 and 8), (b) *Supp. fig. 3(a)* showing 12-MeV DD (*KK*=9 and 10), and (c) *Supp. fig. 1(d)* showing 18-MeV DD (*KK*=11 and 12), as listed in Supplementary Table 1. Further details are the same as in Supp. Fig. 9.

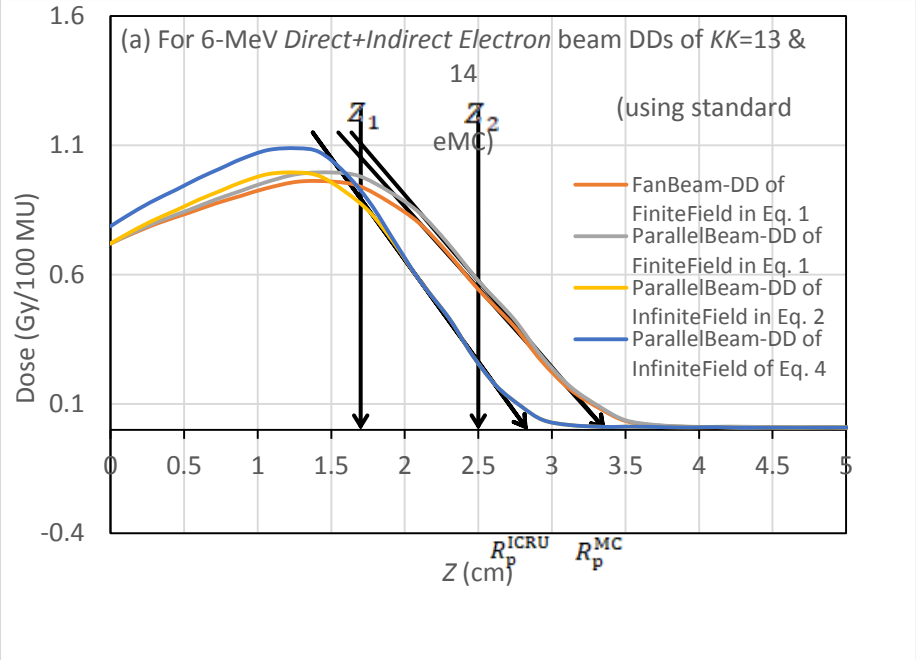
(a) For 6-MeV Direct+Indirect Electron beam DDs of KK=13 & 14 (using standard eMC)
Z_1
Z_2
FanBeam-DD of FiniteField in Eq. 1
ParallelBeam-DD of FiniteField in Eq. 1
ParallelBeam-DD of InfiniteField in Eq. 2
ParallelBeam-DD of InfiniteField of Eq. 4
Dose (Gy/100 MU)
1.6
1.1
0.6
0.1
-0.4
0
0.5
1
1.5
2
2.5
3
3.5
4
4.5
5
R_p^{ICRU}
R_p^{MC}
Z (cm)

(a)

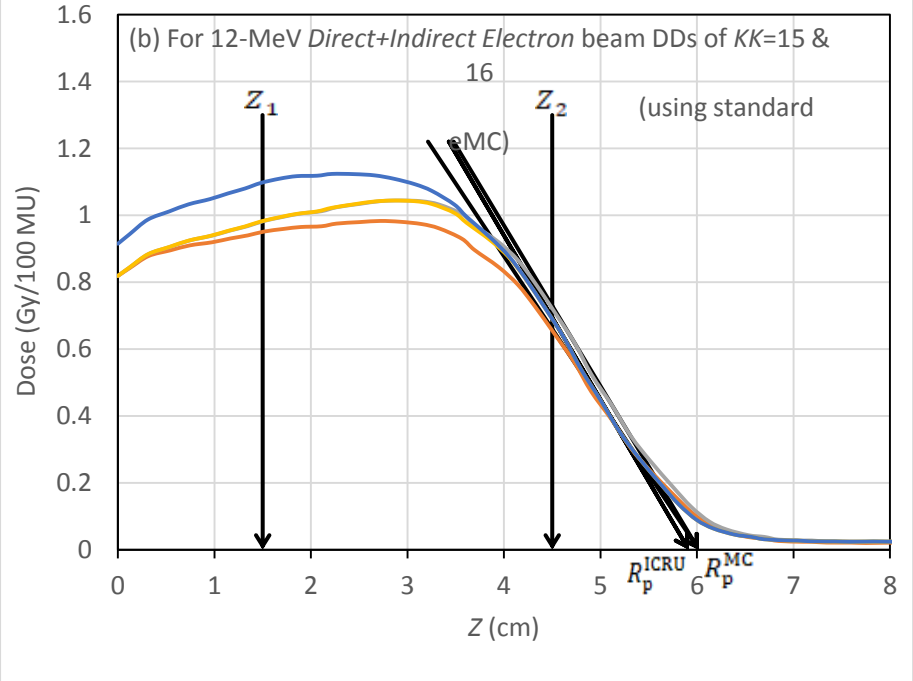
(b) For 12-MeV Direct+Indirect Electron beam DDs of KK=15 & 16 (using standard eMC)
Z_1
Z_2
Dose (Gy/100 MU)
1.6
1.4
1.2
1
0.8
0.6
0.4
0.2
0
0
1
2
3
4
5
6
7
8
R_p^{ICRU}
R_p^{MC}
Z (cm)

(b)

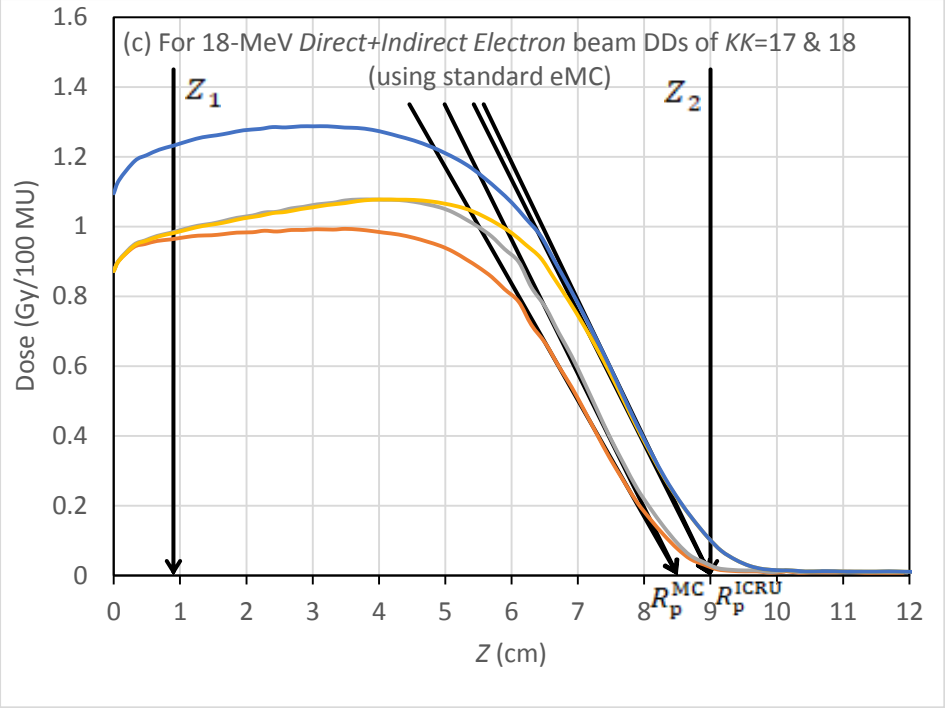

(c)

Supplementary Figure 11a-c Each of (a)-(c) diagrams showing a series of DD curves yielded using the standard eMC, reaching the corresponding parallel beam DD curve of infinite field ($A_0 = \infty$) used for direct-plus-indirect electron beams, derived on the basis of the stepped DD-curves in (a) *Supp. fig. 1(a)* showing 6-MeV DD (*KK*=13 and 14), (b) *Supp. fig. 3(a)* showing 12-MeV DD (*KK*=15 and 16), and (c) *Supp. fig. 1(d)* showing 18-MeV DD (*KK*=17 and 18), as listed in Supplementary Table 1. Further details are the same as in Supp. Fig. 9.

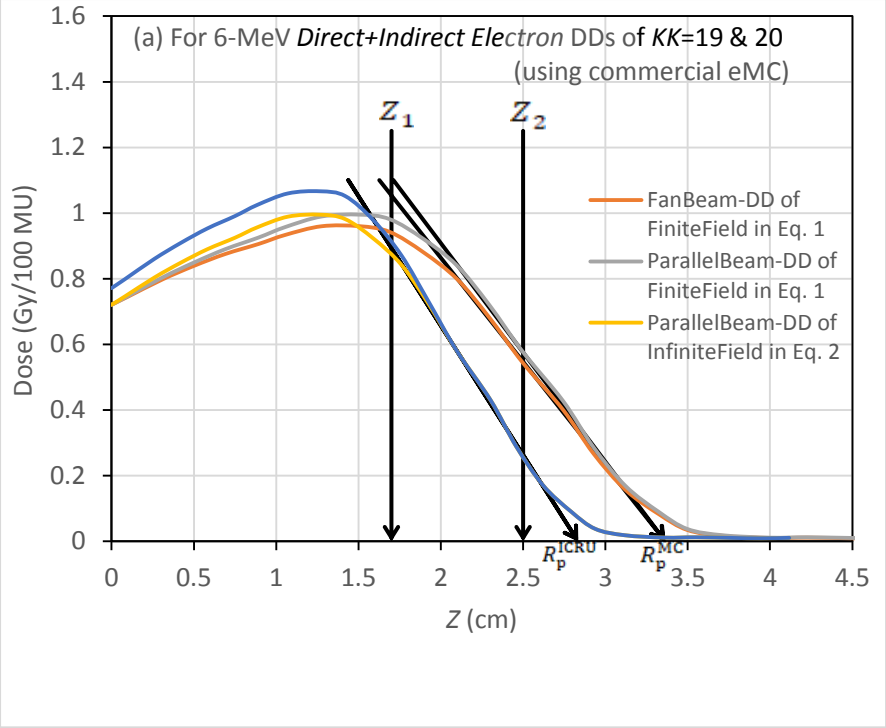
(a) For 6-MeV Direct+Indirect Electron DDs of KK=19 & 20
(using commercial eMC)
Z_1
Z_2
FanBeam-DD of FiniteField in Eq. 1
ParallelBeam-DD of FiniteField in Eq. 1
ParallelBeam-DD of InfiniteField in Eq. 2
R_p^{ICRU}
R_p^{MC}
Dose (Gy/100 MU)
Z (cm)

(a)

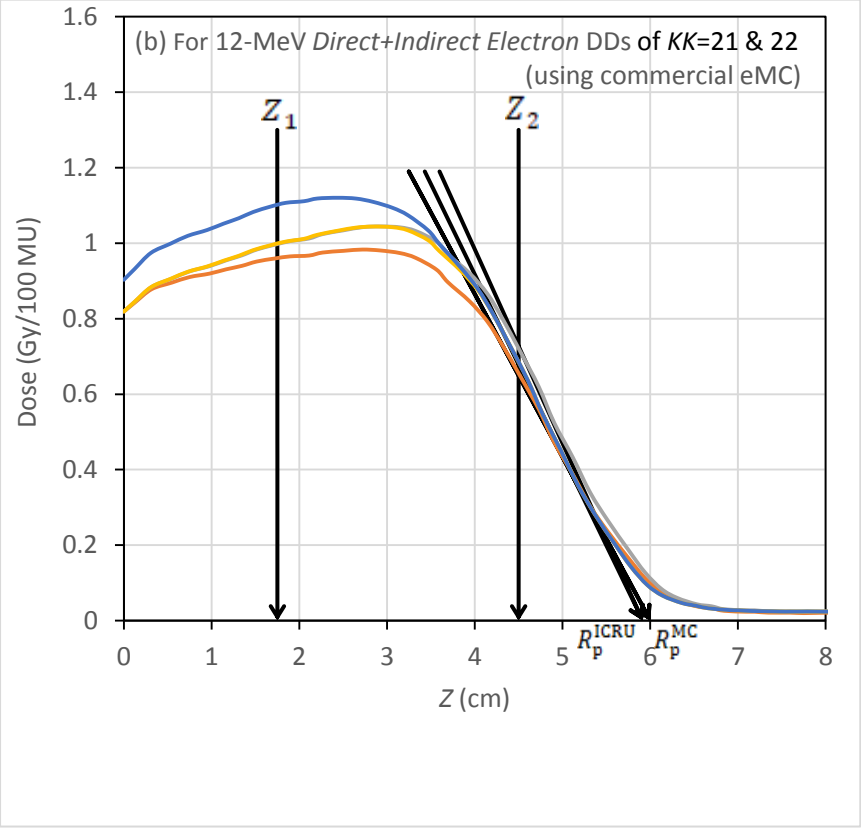
(b) For 12-MeV Direct+Indirect Electron DDs of KK=21 & 22
(using commercial eMC)
Z_1
Z_2
R_p^{ICRU}
R_p^{MC}
Dose (Gy/100 MU)
Z (cm)

(b)

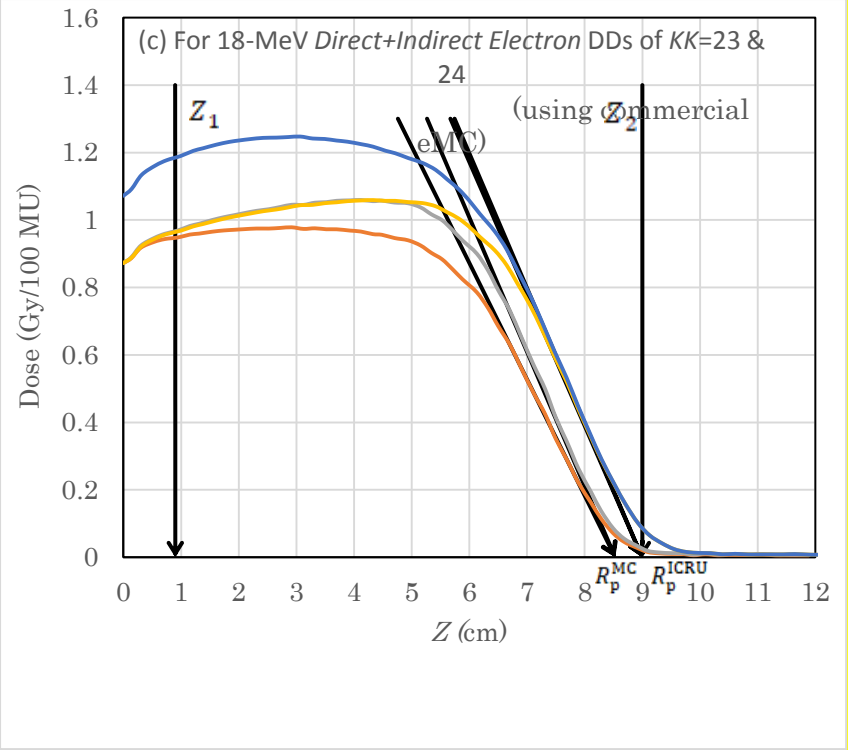

(c)

Supplementary Figure 12a-c Each of (a)-(c) diagrams showing a series of DD curves yielded using the commercial eMC, reaching the corresponding parallel beam DD curve of infinite field ($A_0 = \infty$) used for direct-plus-indirect electron beams, derived on the basis of the stepped DD-curves in (a) *Supp. fig. 1(a)* showing 6-MeV DD (*KK*=19 and 20), (b) *Supp. fig. 3(a)* showing 12-MeV DD (*KK*=21 and 22), and (c) *Supp. fig. 1(d)* showing 18-MeV DD (*KK*=23 and 24), as listed in Supplementary Table 1. Further details are the same as in Supp. Fig. 9.

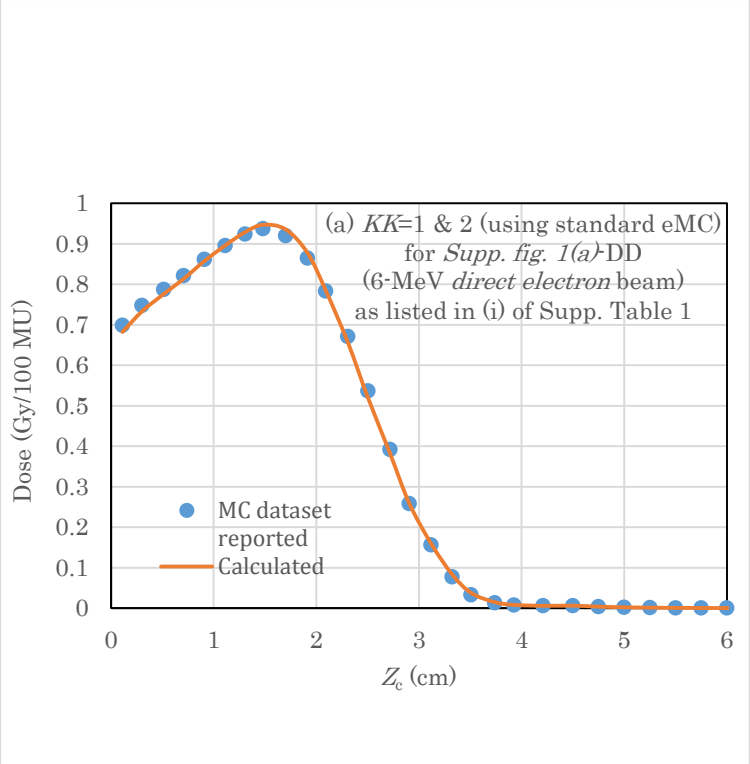
(a) KK=1 & 2 (using standard eMC)
for Supp. fig. 1(a)-DD
(6-MeV direct electron beam)
as listed in (i) of Supp. Table 1
MC dataset
reported
Calculated
Dose (Gy/100 MU)
Zc (cm)

(a)

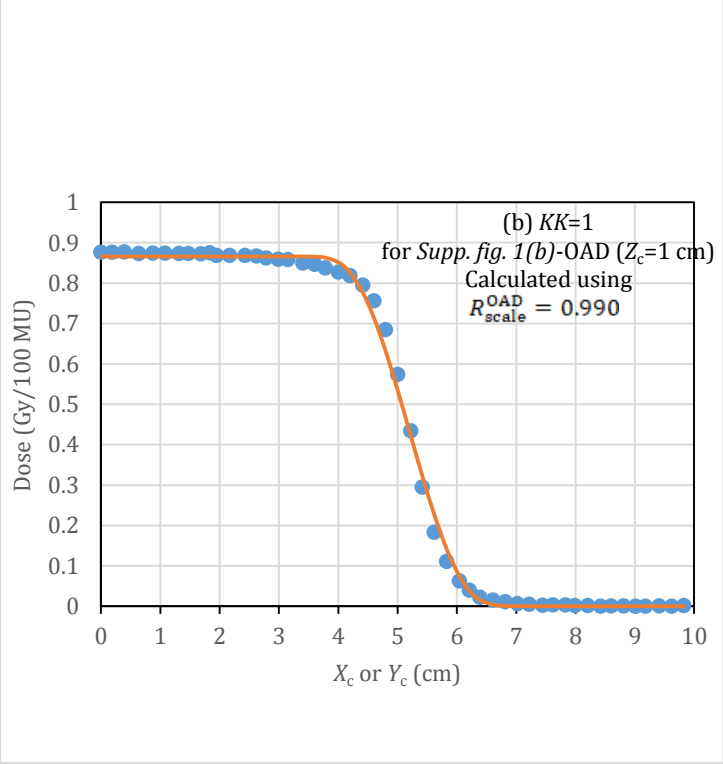
(b) KK=1
for Supp. fig. 1(b)-OAD (Zc=1 cm)
Calculated using
R_scale^OAD = 0.990
Dose (Gy/100 MU)
Xc or Yc (cm)

(b)

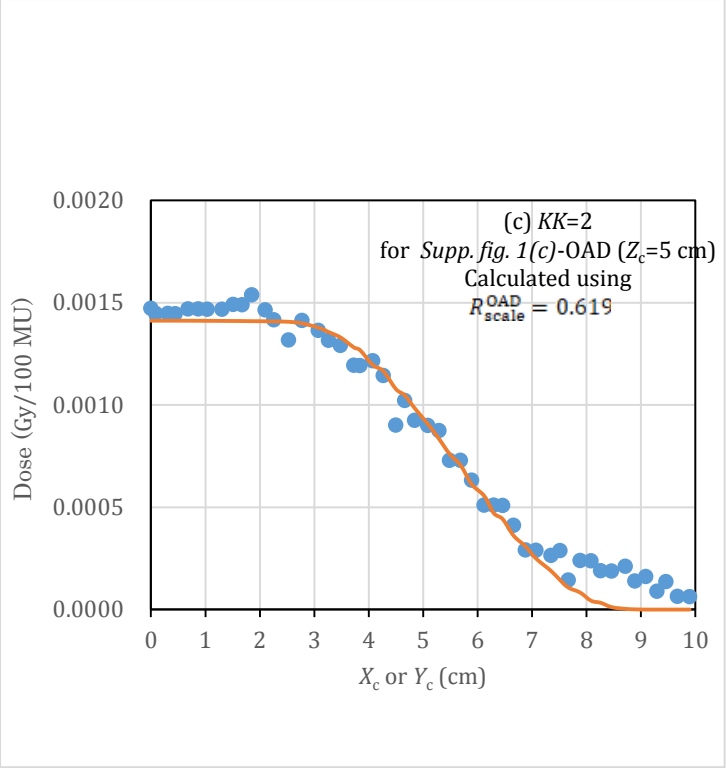

(c)

Supplementary Figure 13a-c One DD dataset in (a) and two OAD datasets on planes of (b) $Z_c = 1$ cm and (c) $Z_c = 5$ cm are illustrated for the 6-MeV *direct electron* beam, indicating *KK*=1 and 2 listed in (i) of Supplementary Table 1. Dots show the dose results with the standard eMC; and lines, the calculated dose results.

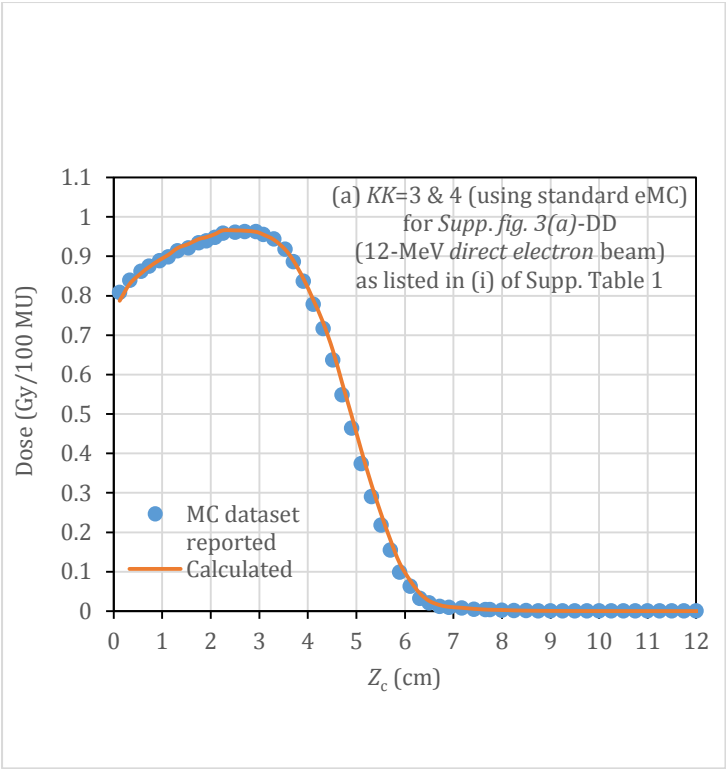
(a) KK=3 & 4 (using standard eMC)
for Supp. fig. 3(a)-DD
(12-MeV direct electron beam)
as listed in (i) of Supp. Table 1
MC dataset
reported
Calculated
Dose (Gy/100 MU)
Z_c (cm)

(a)

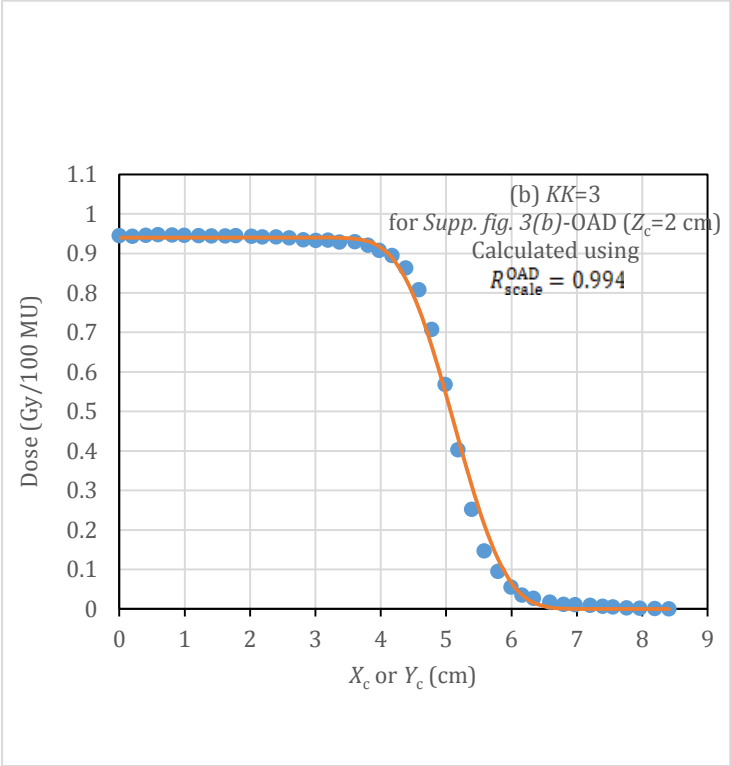
(b) KK=3
for Supp. fig. 3(b)-OAD (Z_c=2 cm)
Calculated using
$R_{scale}^{OAD} = 0.994$
Dose (Gy/100 MU)
X_c or Y_c (cm)

(b)

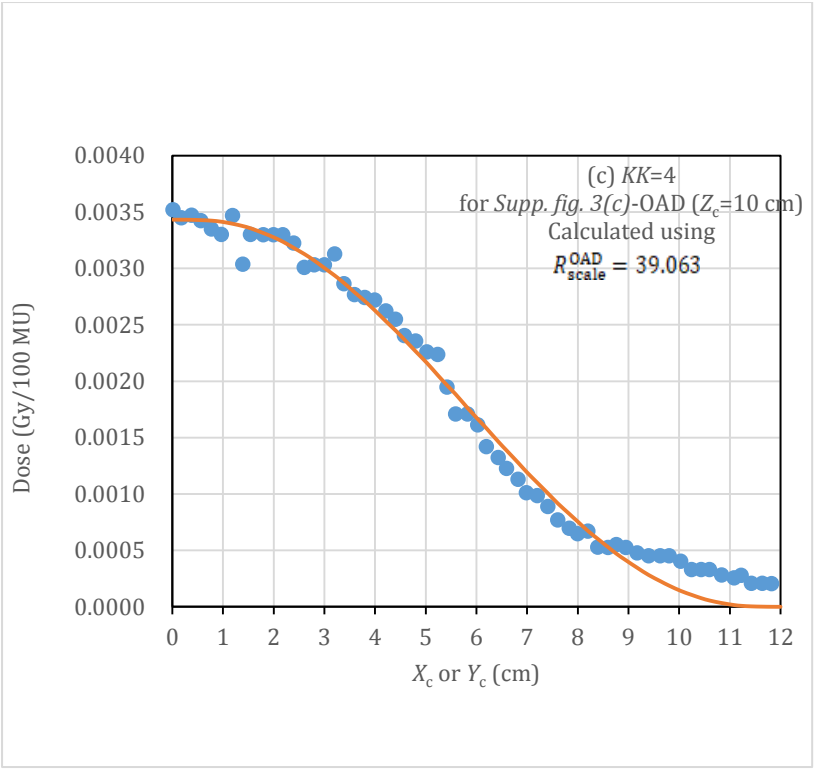

(c)

Supplementary Figure 14a-c One DD dataset in (a) and two OAD datasets on planes of (b) $Z_c = 2$ cm and (c) $Z_c = 10$ cm are illustrated for the 12-MeV *direct electron* beam, indicating *KK*=3 and 4 listed in (i) of Supplementary Table 1. Further details are the same as in Supp. Fig. 13.

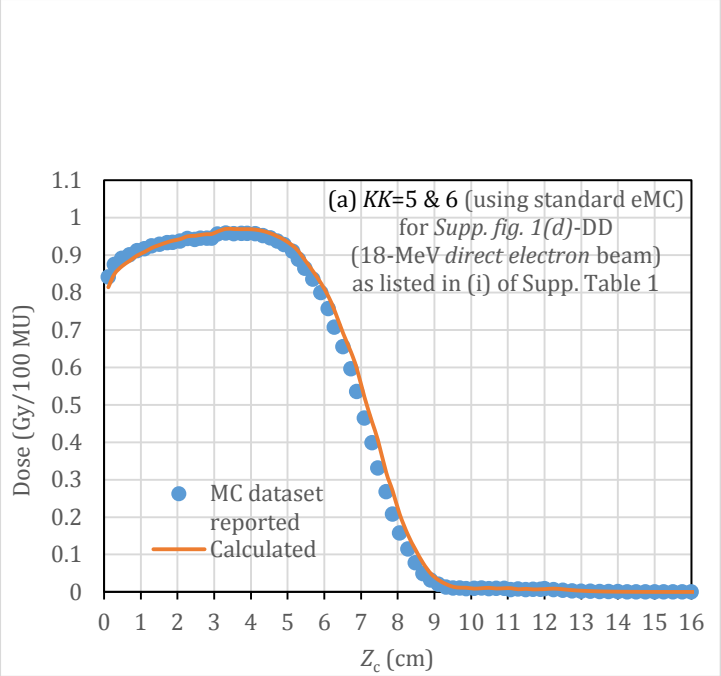
(a) KK=5 & 6 (using standard eMC)
for Supp. fig. 1(d)-DD
(18-MeV direct electron beam)
as listed in (i) of Supp. Table 1
MC dataset
reported
Calculated
Dose (Gy/100 MU)
Zc (cm)

(a)

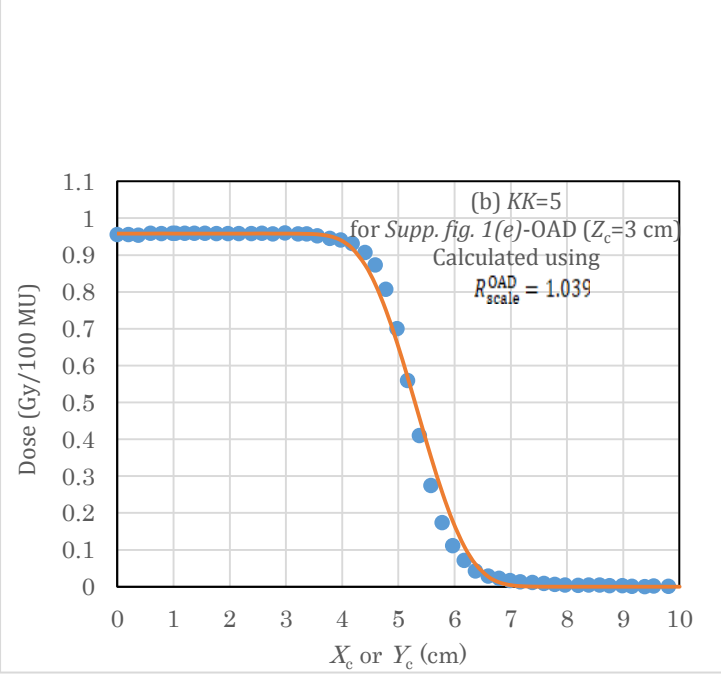
(b) KK=5
for Supp. fig. 1(e)-OAD (Zc=3 cm)
Calculated using
R_{scale}^{OAD} = 1.039
Dose (Gy/100 MU)
Xc or Yc (cm)

(b)

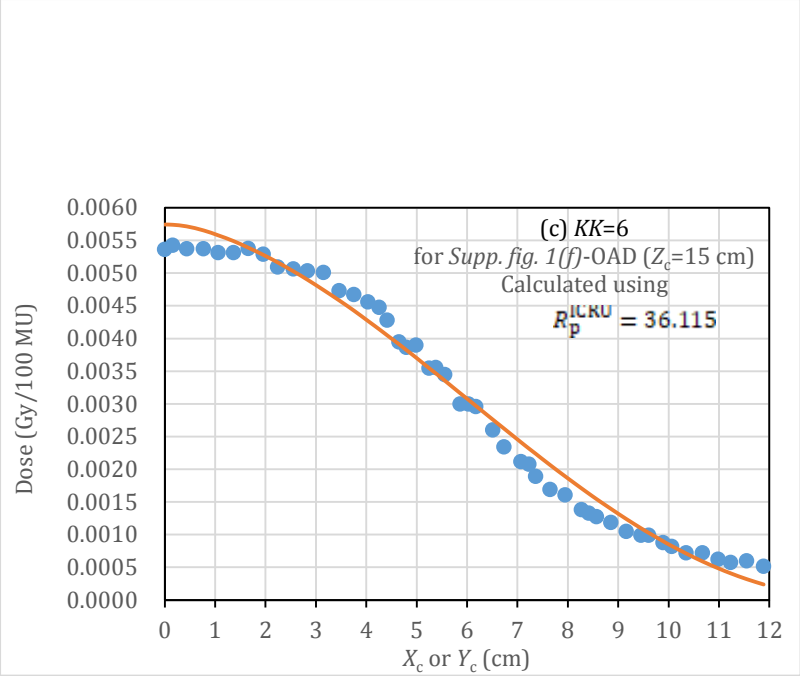

(c)

Supplementary Figure 15a-c One DD dataset in (a) and two OAD datasets on planes of (b) $Z_c = 3$ cm and (c) $Z_c = 15$ cm are illustrated for the 18-MeV *direct electron* beam, indicating *KK*=5 and 6 listed in (i) of Supplementary Table 1. Further details are the same as in Supp. Fig. 13.

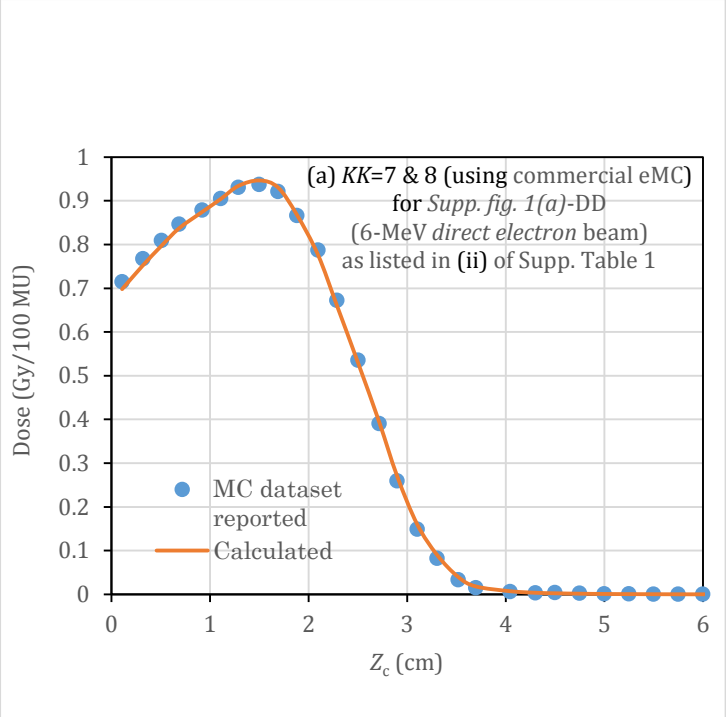
(a) KK=7 & 8 (using commercial eMC)
for Supp. fig. 1(a)-DD
(6-MeV direct electron beam)
as listed in (ii) of Supp. Table 1
MC dataset reported
Calculated
Dose (Gy/100 MU)
Z_c (cm)

(a)

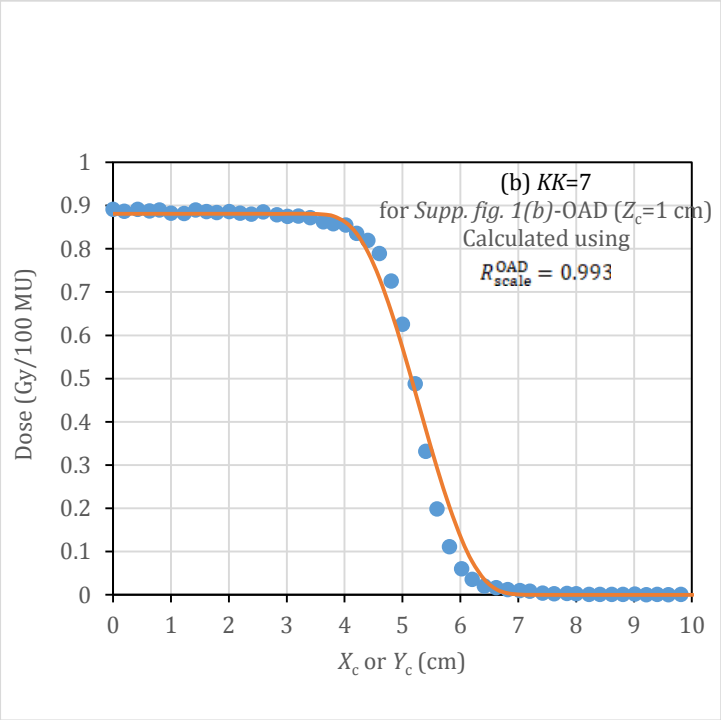
(b) KK=7
for Supp. fig. 1(b)-OAD (Z_c=1 cm)
Calculated using
$R_{scale}^{OAD} = 0.993$
Dose (Gy/100 MU)
X_c or Y_c (cm)

(b)

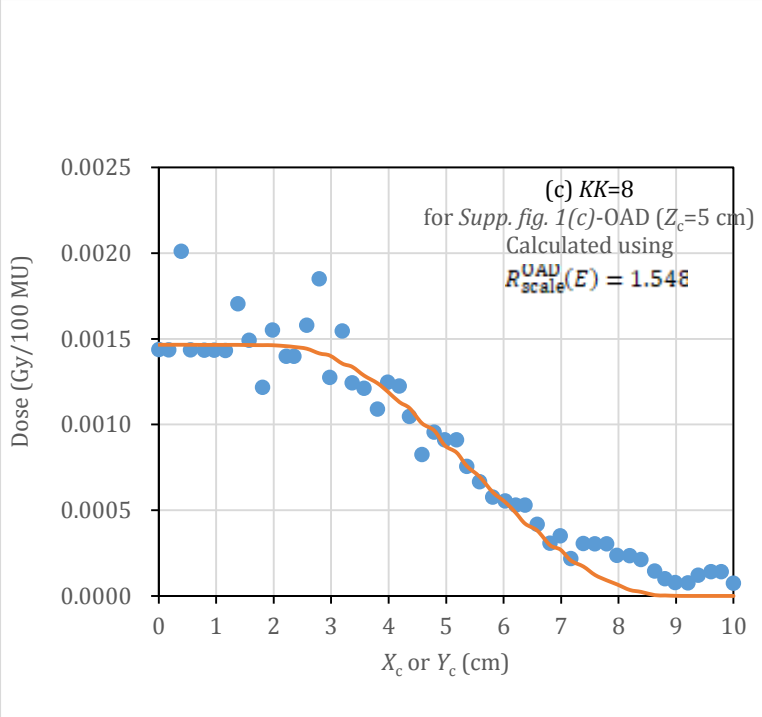

(c)

Supplementary Figure 16a-c One DD dataset in (a) and two OAD datasets on planes of (b) $Z_c = 1$ cm and (c) $Z_c = 5$ cm are illustrated for the 6-MeV *direct electron* beam, indicating *KK*=7 and 8 listed in (ii) of Supplementary Table 1. Dots show the dose results with the commercial eMC; and lines, the calculated dose results.

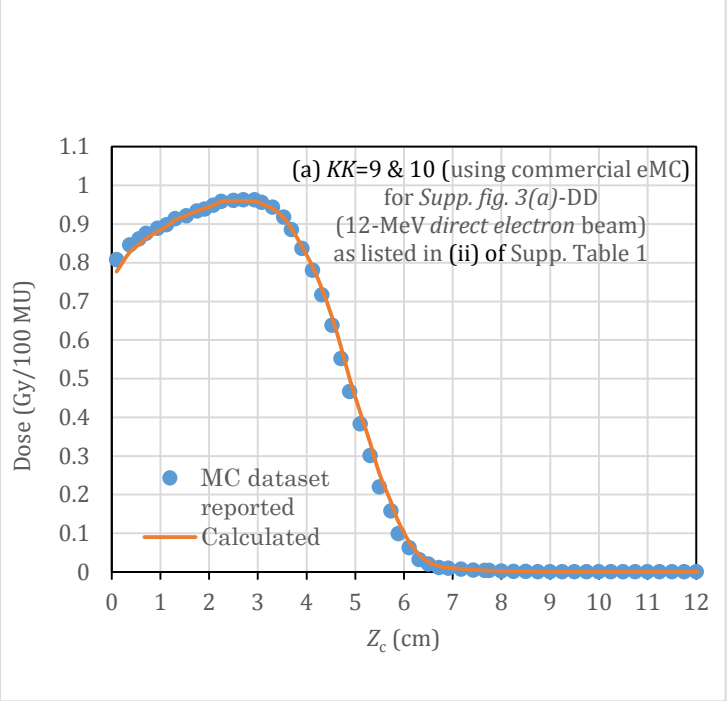
(a) KK=9 & 10 (using commercial eMC)
for Supp. fig. 3(a)-DD
(12-MeV direct electron beam)
as listed in (ii) of Supp. Table 1
MC dataset reported
Calculated
Dose (Gy/100 MU)
Zc (cm)

(a)

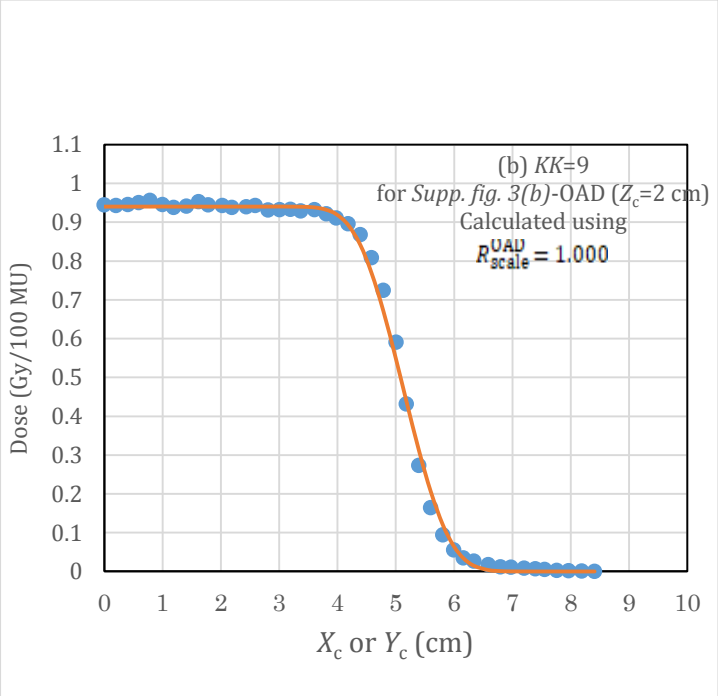
(b) KK=9
for Supp. fig. 3(b)-OAD (Zc=2 cm)
Calculated using
$R_{scale}^{OAD} = 1.000$
Dose (Gy/100 MU)
Xc or Yc (cm)

(b)

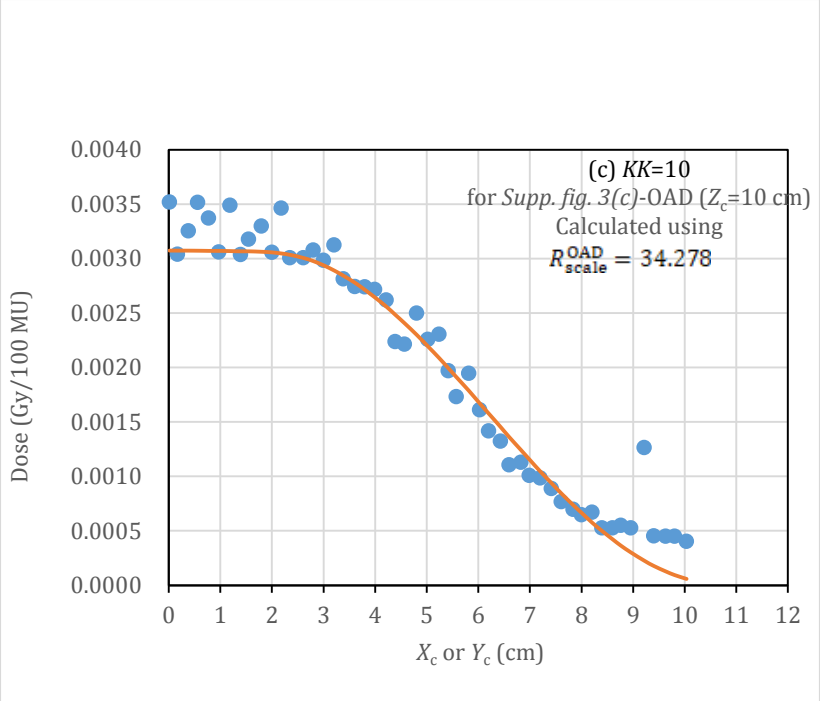

(c)

Supplementary Figure 17a-c One DD dataset in (a) and two OAD datasets on planes of (b) $Z_c = 2\,\mathrm{cm}$ and (c) $Z_c = 10\,\mathrm{cm}$ are illustrated for the 12-MeV *direct electron* beam, indicating *KK*=9 and 10 listed in (ii) of Supplementary Table 1. Further details are the same as in Supp. Fig. 16.

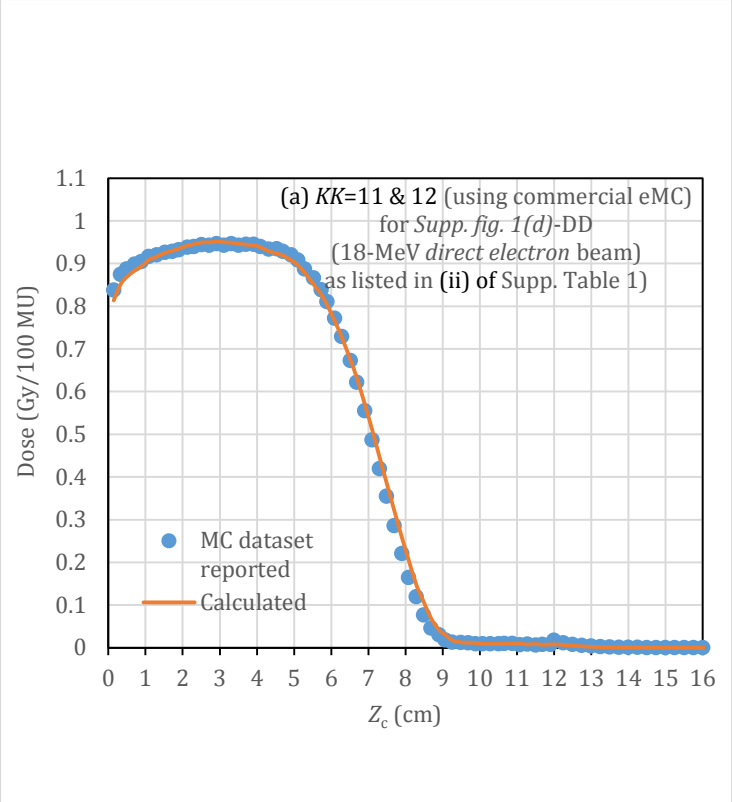
(a) KK=11 & 12 (using commercial eMC)
for Supp. fig. 1(d)-DD
(18-MeV direct electron beam)
as listed in (ii) of Supp. Table 1)
MC dataset
reported
Calculated
Dose (Gy/100 MU)
Z_c (cm)

(a)

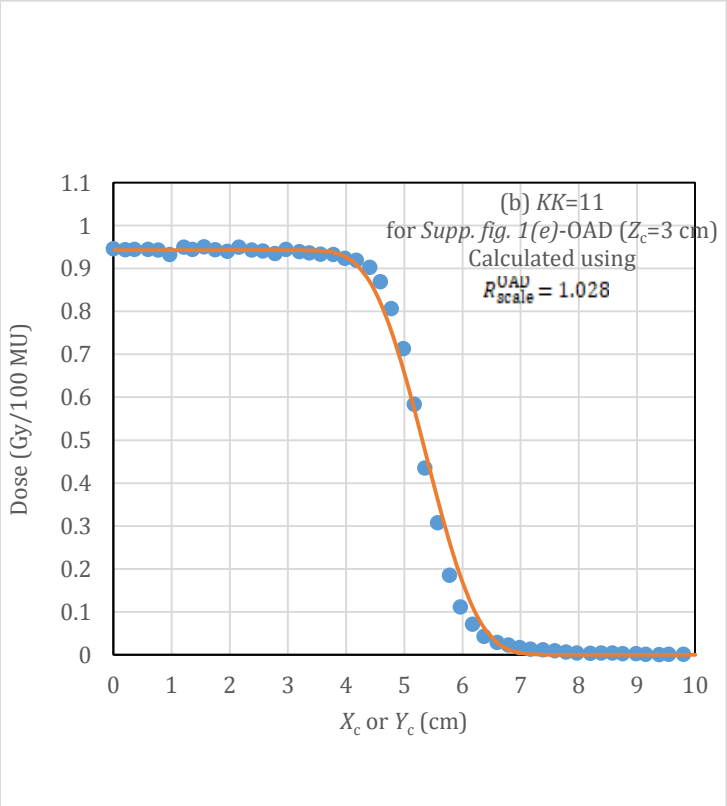
(b) KK=11
for Supp. fig. 1(e)-OAD (Z_c=3 cm)
Calculated using
$R_{scale}^{OAD} = 1.028$
Dose (Gy/100 MU)
X_c or Y_c (cm)

(b)

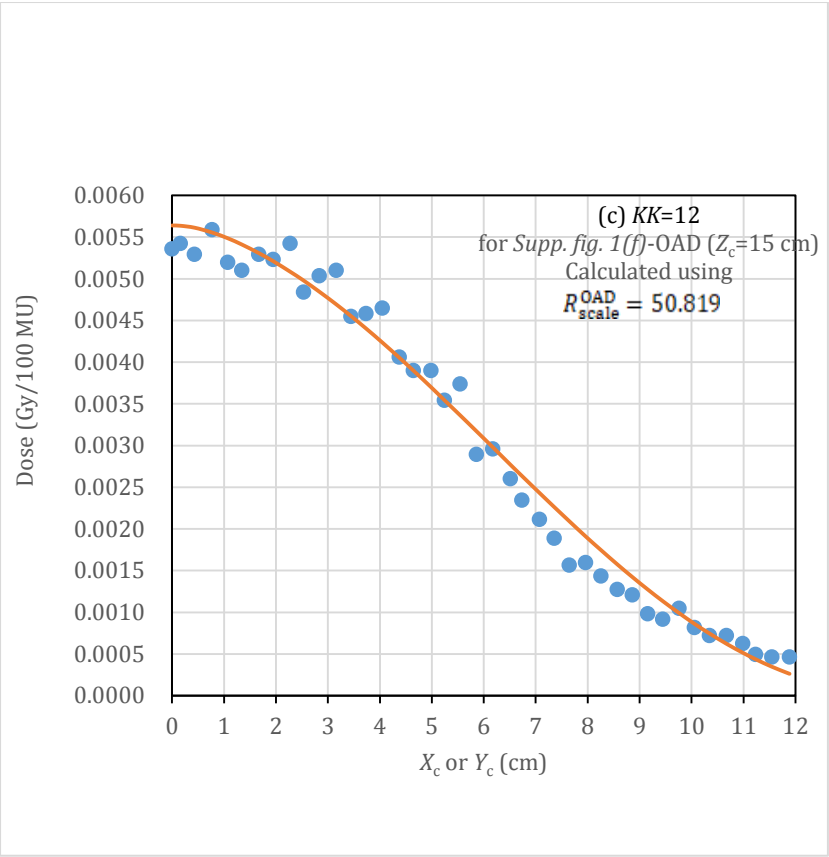

(c)

Supplementary Figure 18a-c One DD dataset in (a) and two OAD datasets on planes of (b) $Z_c = 3$ cm and (c) $Z_c = 15$ cm are illustrated for the 18-MeV *direct electron* beam, indicating *KK*=11 and 12 listed in (ii) of Supplementary Table 1. Further details are the same as in Supp. Fig. 16.

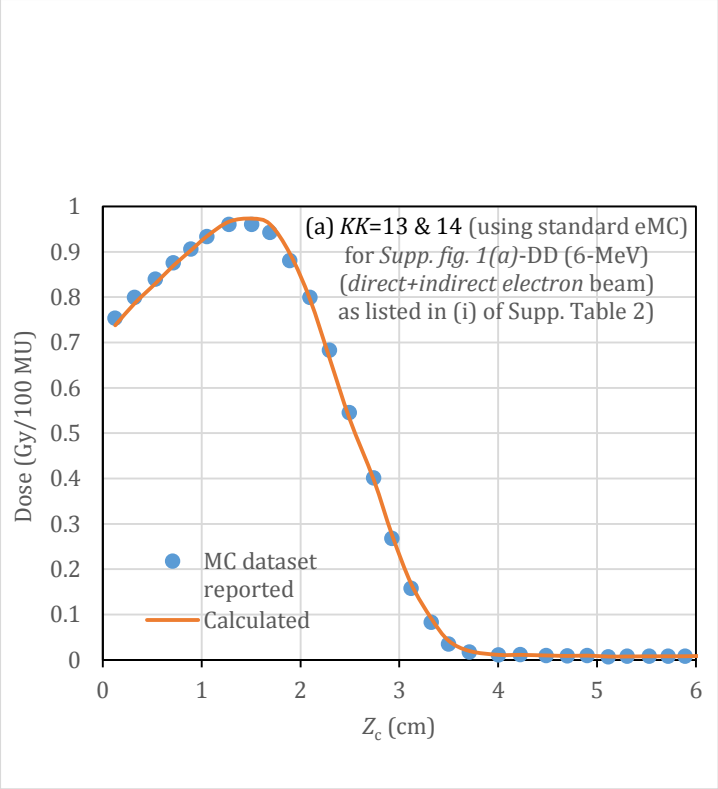
(a) KK=13 & 14 (using standard eMC)
for Supp. fig. 1(a)-DD (6-MeV)
(direct+indirect electron beam)
as listed in (i) of Supp. Table 2)
MC dataset
reported
Calculated
Dose (Gy/100 MU)
Z_c (cm)

(a)

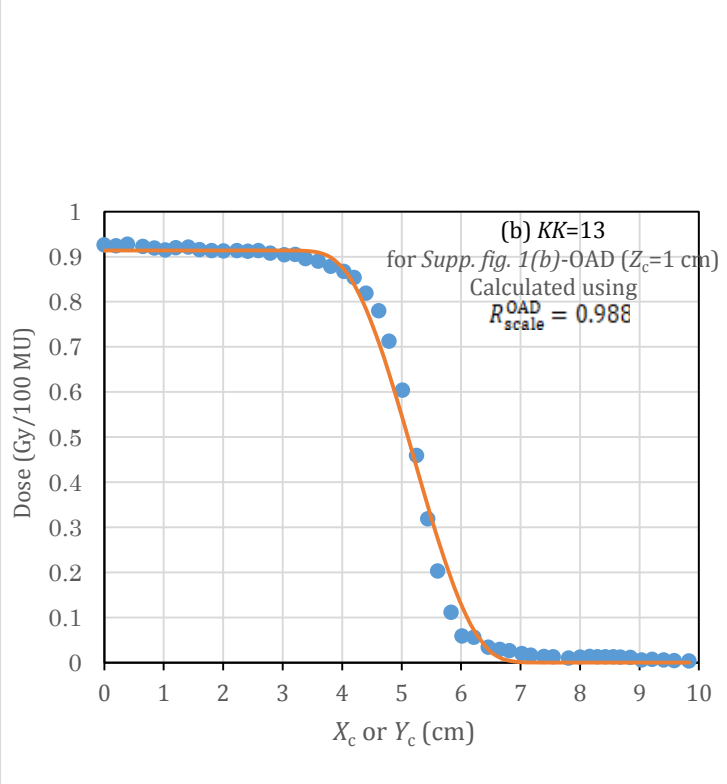
(b) KK=13
for Supp. fig. 1(b)-OAD (Z_c=1 cm)
Calculated using
$R_{scale}^{OAD} = 0.988$
Dose (Gy/100 MU)
X_c or Y_c (cm)

(b)

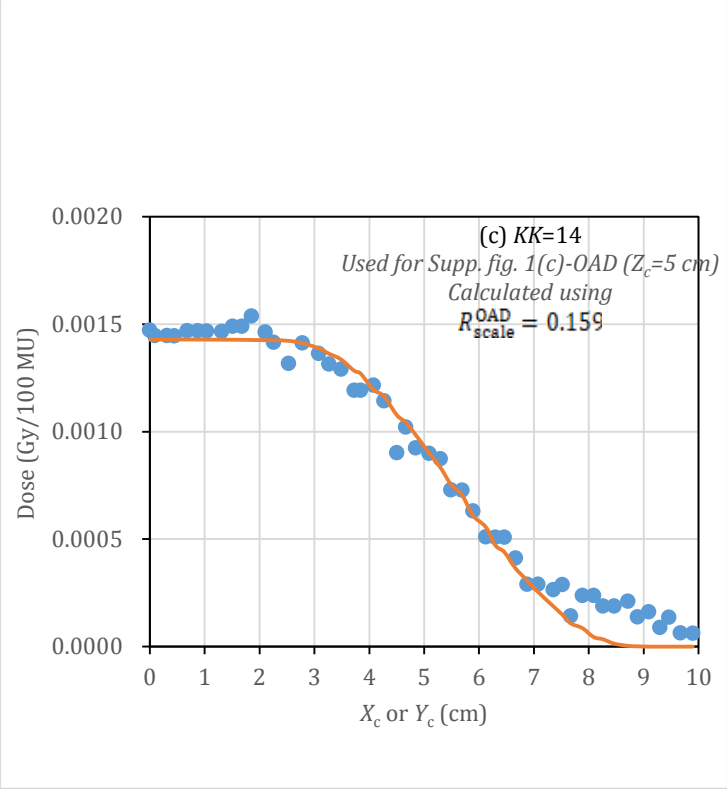

(c)

Supplementary Figure 19a-c One DD dataset in (a) and two OAD datasets on planes of (b) $Z_c = 1$ cm and (c) $Z_c = 5$ cm are illustrated for the 6-MeV *direct-plus-indirect electron* beam, indicating *KK*=13 and 14 listed in (i) of Supplementary Table 1. Dots show the dose results using the standard eMC; and lines, the calculated dose results.

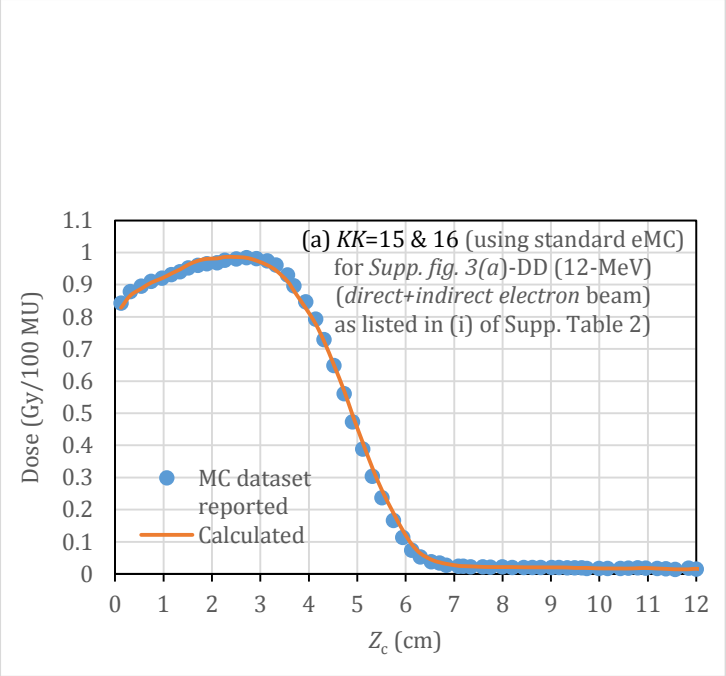
(a) KK=15 & 16 (using standard eMC)
for Supp. fig. 3(a)-DD (12-MeV)
(direct+indirect electron beam)
as listed in (i) of Supp. Table 2)
MC dataset reported
Calculated
Dose (Gy/100 MU)
Zc (cm)

(a)

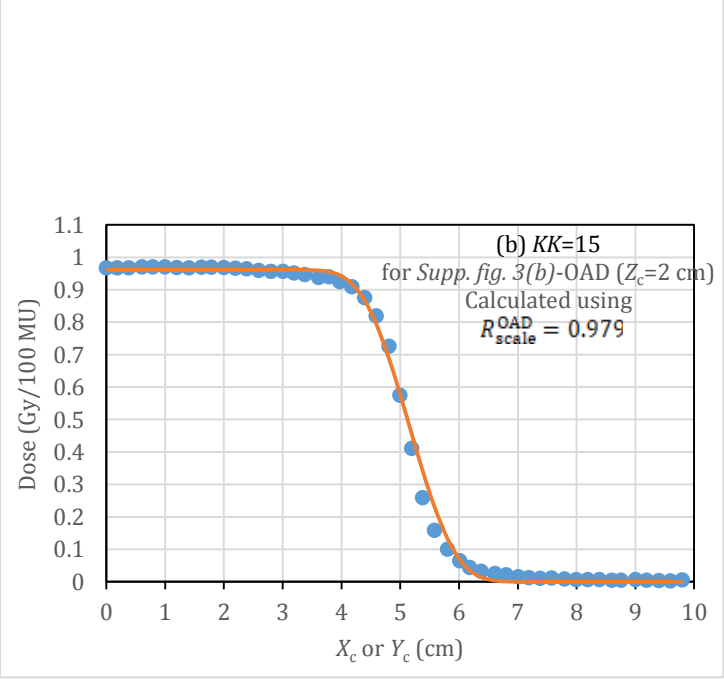
(b) KK=15
for Supp. fig. 3(b)-OAD (Zc=2 cm)
Calculated using
$R_{scale}^{OAD} = 0.979$
Dose (Gy/100 MU)
Xc or Yc (cm)

(b)

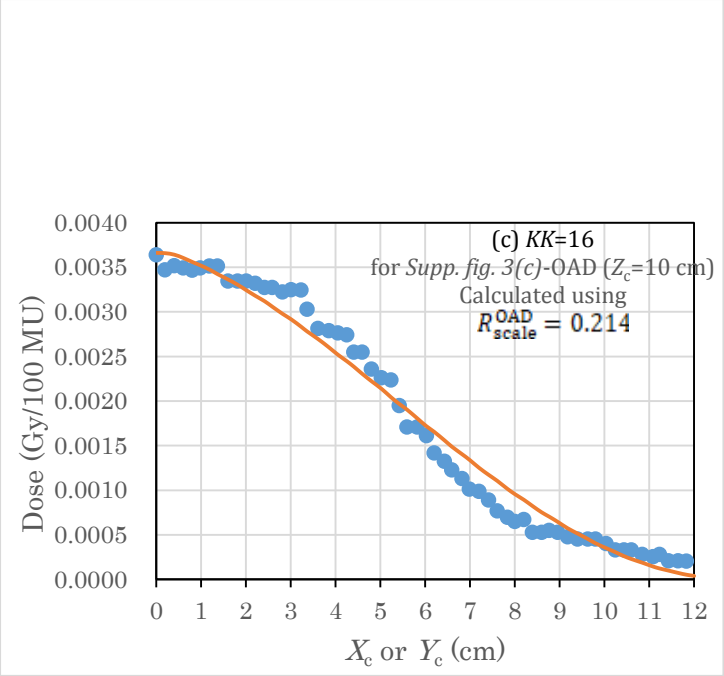

(c)

Supplementary Figure 20a-c One DD dataset in (a) and two OAD datasets on planes of (b) $Z_c = 2$ cm and (c) $Z_c = 10$ cm are illustrated for the 6-MeV *direct-plus-indirect electron* beam, indicating *KK*=13 and 14 listed in (i) of Supplementary Table 2. Further details are the same as in Supp. Fig. 19.

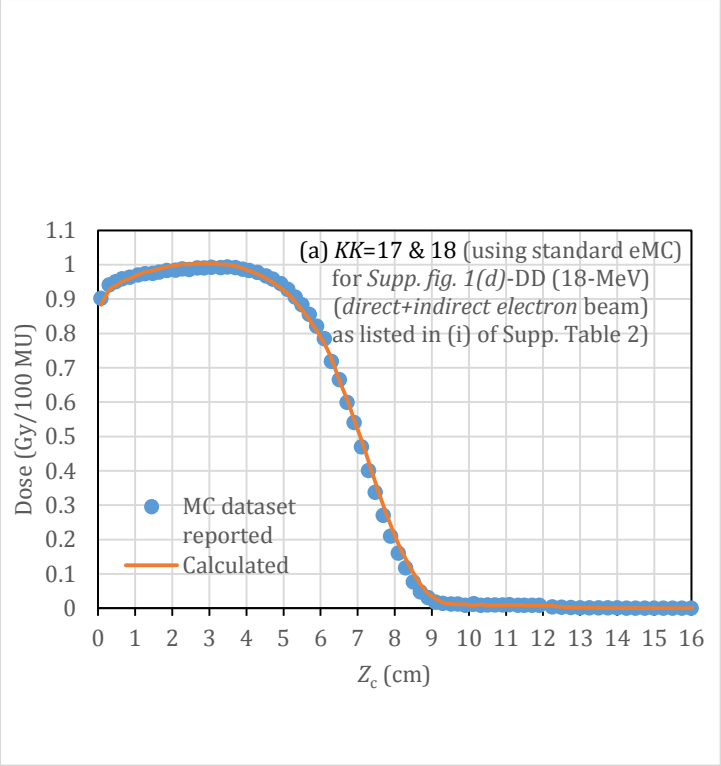
(a) KK=17 & 18 (using standard eMC)
for Supp. fig. 1(d)-DD (18-MeV)
(direct+indirect electron beam)
as listed in (i) of Supp. Table 2)
MC dataset reported
Calculated
Dose (Gy/100 MU)
Z_c (cm)

(a)

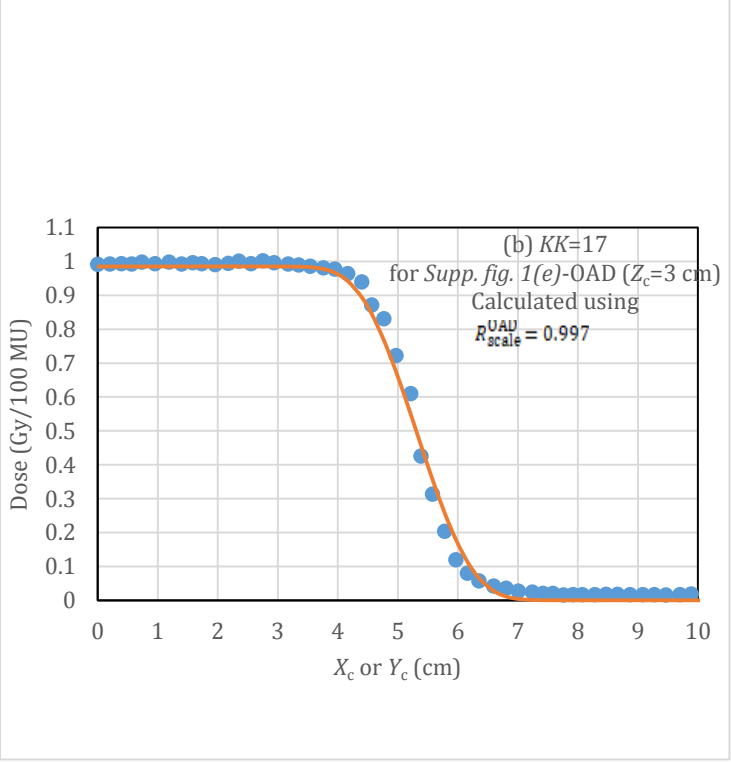
(b) KK=17
for Supp. fig. 1(e)-OAD (Z_c=3 cm)
Calculated using
$R_{scale}^{OAD} = 0.997$
Dose (Gy/100 MU)
X_c or Y_c (cm)

(b)

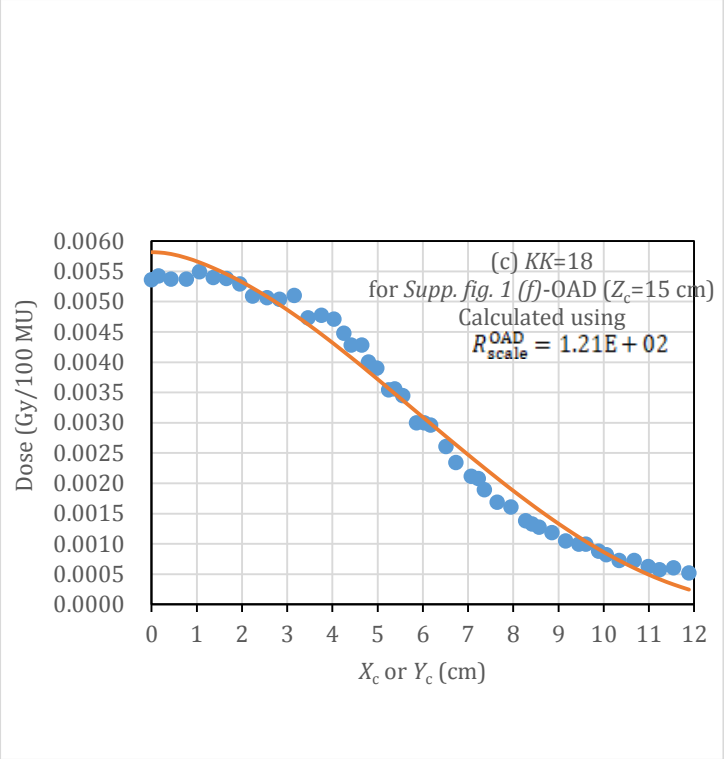

(c)

Supplementary Figure 21a-c One DD dataset in (a) and two OAD datasets on planes of (b) $Z_c = 3$ cm and (c) $Z_c = 15$ cm are illustrated for the 18-MeV *direct-plus-indirect electron* beam, indicating *KK*=17 and 18 listed in (i) of Supplementary Table 2. Further details are the same as in Supp. Fig. 19.

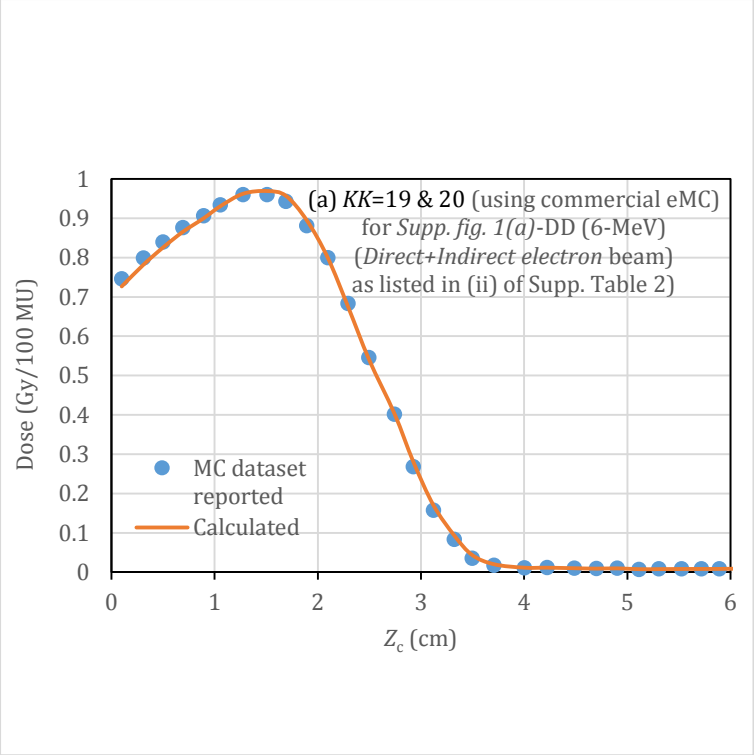
(a) KK=19 & 20 (using commercial eMC)
for Supp. fig. 1(a)-DD (6-MeV)
(Direct+Indirect electron beam)
as listed in (ii) of Supp. Table 2)
MC dataset reported
Calculated
Dose (Gy/100 MU)
Zc (cm)

(a)

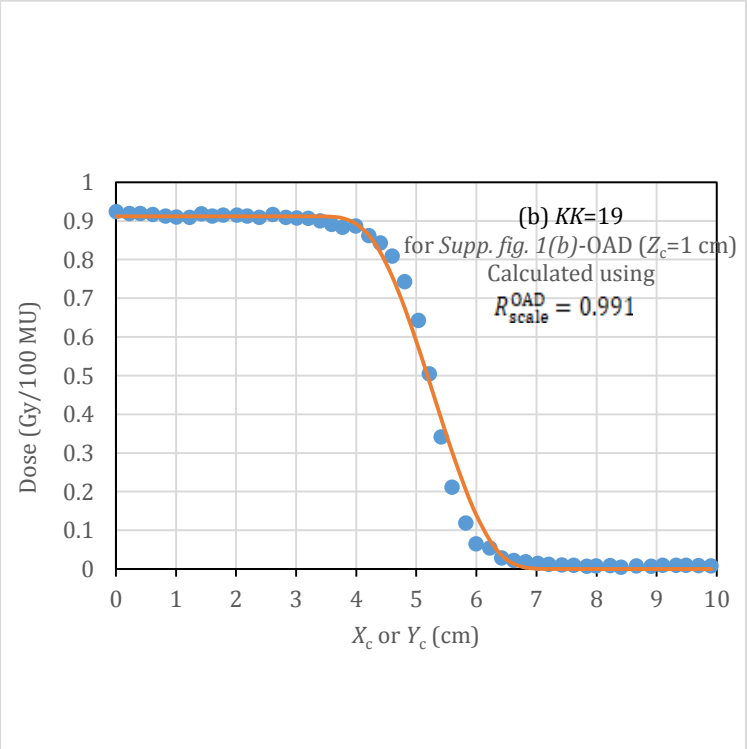
(b) KK=19
for Supp. fig. 1(b)-OAD (Zc=1 cm)
Calculated using
$R_{scale}^{OAD} = 0.991$
Dose (Gy/100 MU)
Xc or Yc (cm)

(b)

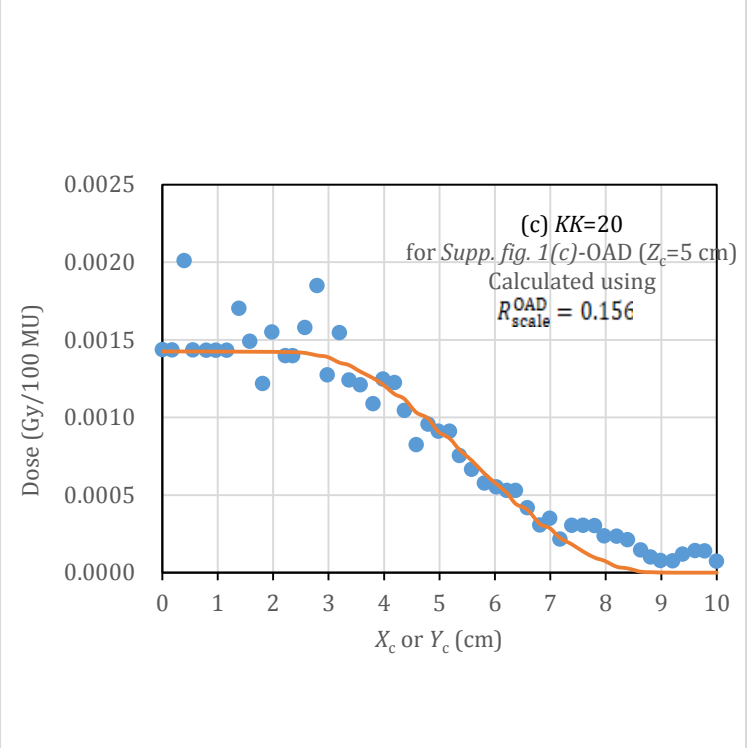

(c)

Supplementary Figure 22a-c One DD dataset in (a) and two OAD datasets on planes of (b) $Z_c = 1$ cm and (c) $Z_c = 5$ cm are illustrated for the 6-MeV *direct-plus-indirect electron* beam, indicating *KK*=19 and 20 listed in (ii) of Supplementary Table 2. Dots show the dose results of the commercial eMC; and lines, the calculated dose results.

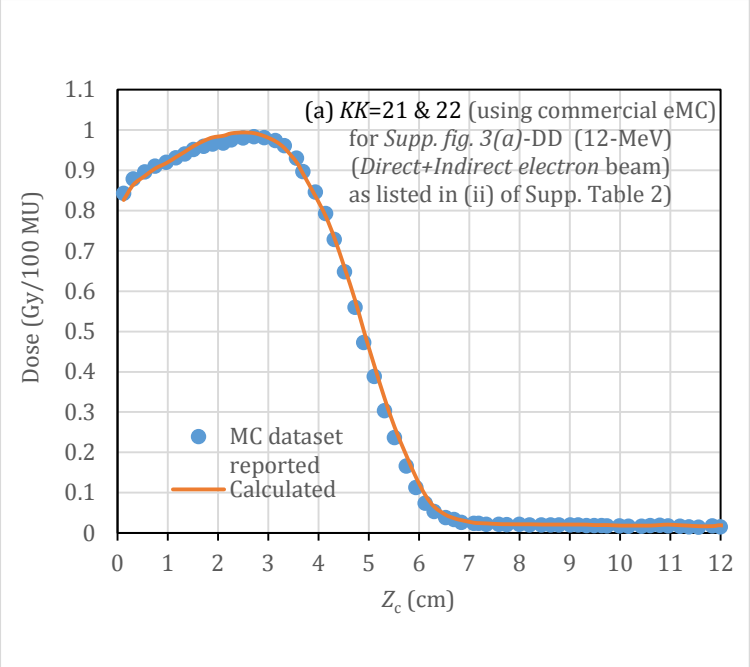
(a) KK=21 & 22 (using commercial eMC)
for Supp. fig. 3(a)-DD (12-MeV)
(Direct+Indirect electron beam)
as listed in (ii) of Supp. Table 2)
MC dataset
reported
Calculated
Dose (Gy/100 MU)
Zc (cm)

(a)

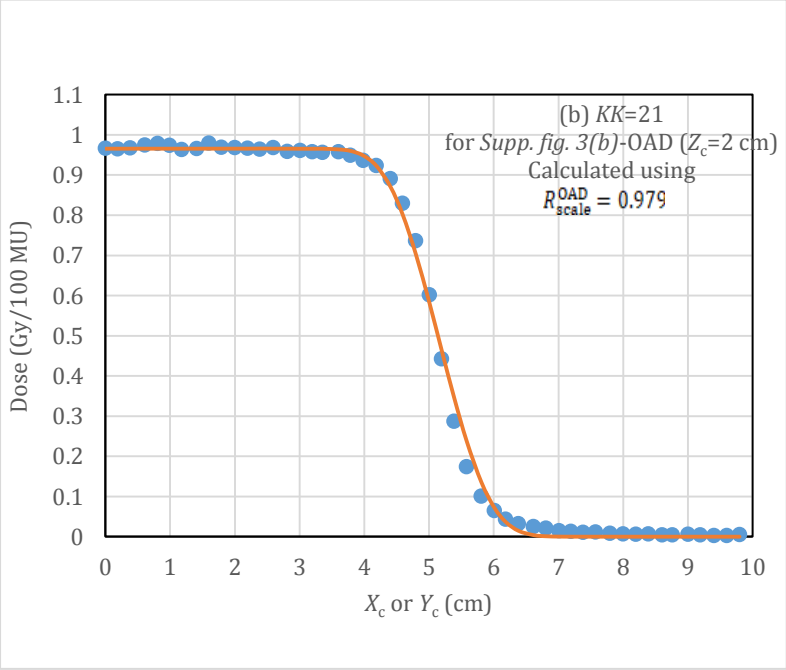
(b) KK=21
for Supp. fig. 3(b)-OAD (Zc=2 cm)
Calculated using
R^OAD_scale = 0.979
Dose (Gy/100 MU)
Xc or Yc (cm)

(b)

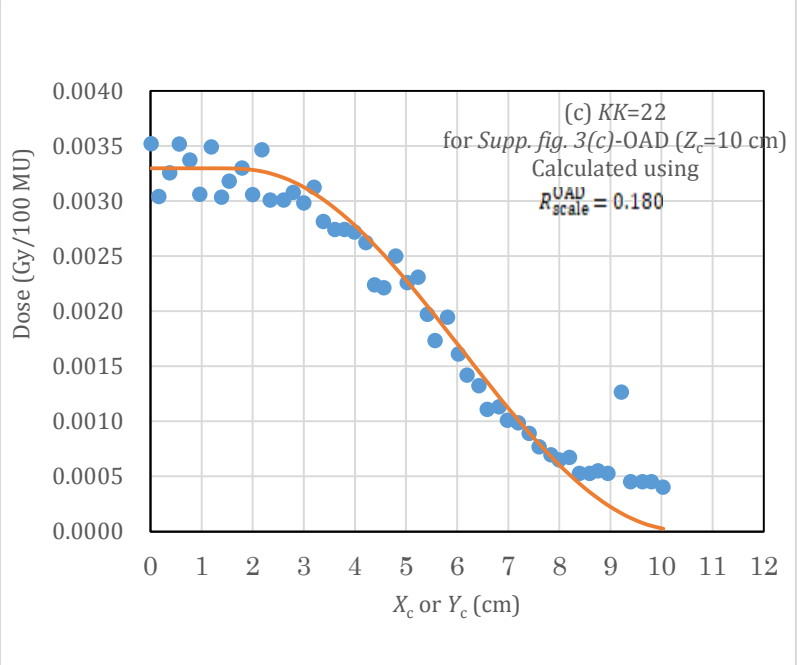

(c)

Supplementary Figure 23a-c One DD dataset in (a) and two OAD datasets on planes of (b) $Z_c = 2$ cm and (c) $Z_c = 10$ cm are illustrated for the 12-MeV *direct-plus-indirect electron* beam, indicating *KK*=21 and 22 listed in (ii) of Supplementary Table 2. Further details are the same as in Supp. Fig. 22.

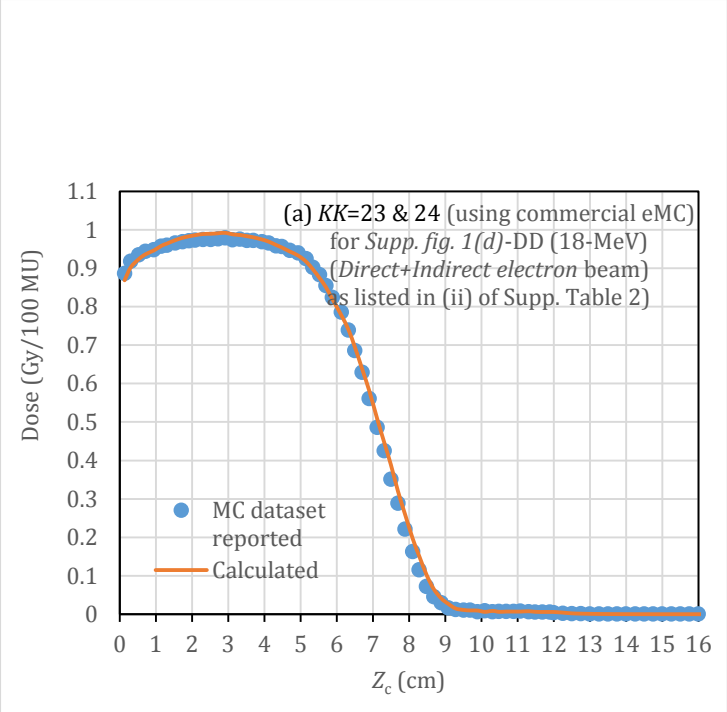
(a) KK=23 & 24 (using commercial eMC)
for Supp. fig. 1(d)-DD (18-MeV)
(Direct+Indirect electron beam)
as listed in (ii) of Supp. Table 2)
MC dataset reported
Calculated
Dose (Gy/100 MU)
Z_c (cm)

(a)

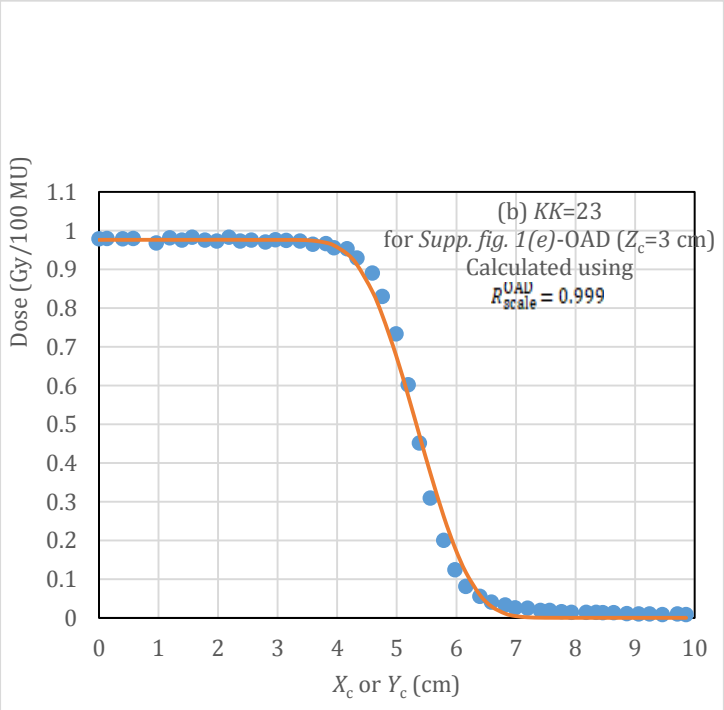
(b) KK=23
for Supp. fig. 1(e)-OAD (Z_c=3 cm)
Calculated using
$R_{scale}^{OAD} = 0.999$
Dose (Gy/100 MU)
X_c or Y_c (cm)

(b)

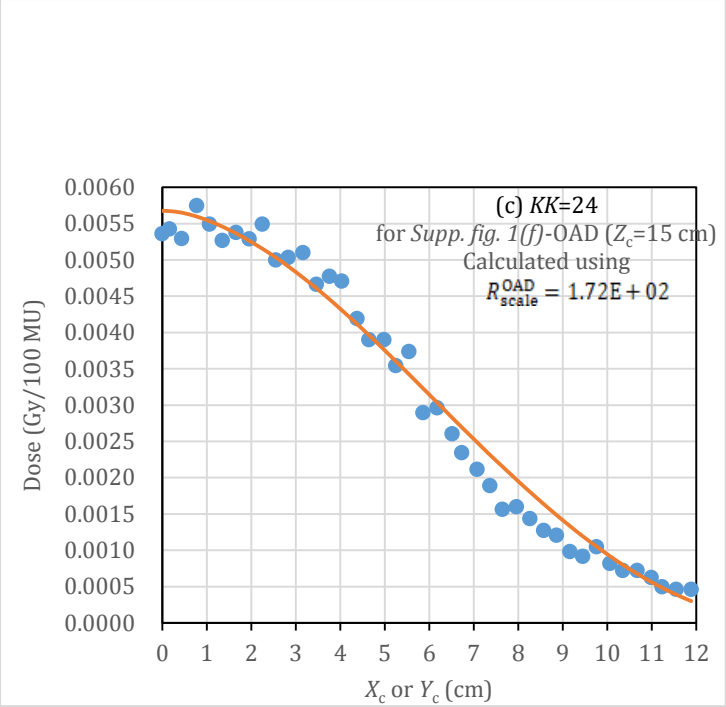

(c)

Supplementary Figure 24a-c One DD dataset in (a) and two OAD datasets on planes of (b) $Z_c = 3$ cm and (c) $Z_c = 15$ cm are illustrated for the 18-MeV *direct-plus-indirect electron* beam, indicating *KK*=23 and 24 listed in (ii) of Supplementary Table 2. Further details are the same as in Supp. Fig. 22.